

# Challenges and progresses of lithium-metal batteries.

WANG, J., GE, B., YANG, M., WANG, J., LIU, D., FERNANDEZ, C., CHEN, X. and PENG, Q.

2021

# Challenges and Progresses of Lithium-Metal Batteries

Jinming Wang<sup>1</sup>, Bingcheng Ge<sup>1</sup>, Hui Li<sup>1</sup>, Meng Yang<sup>1</sup>, Jing Wang<sup>\*1</sup>, Di Liu<sup>1</sup>, Carlos Fernandez<sup>2</sup>, Xiaobo Chen<sup>3</sup>, Qiuming Peng<sup>\*1</sup>

<sup>1</sup> State Key Laboratory of Metastable Materials Science and Technology, Yanshan University, Qinhuangdao 066004, China.

<sup>2</sup> School of Pharmacy and Life Sciences, Robert Gordon University, Aberdeen, AB107GJ, UK

<sup>3</sup> School of Engineering, RMIT University, Carlton 3053, VIC, Australia

**Abstract:** Lithium-metal batteries (LMBs) have received considerable enthusiasm as the candidates for next-generation high energy density storage devices. However, the unexpected electrochemical deposition of metallic Li on the surface of anode has been considered as the major obstacle, severely limiting the practical applications of high-performance LMBs. In this review, we firstly introduce three major challenges impeding large-scale commercial implementation of LMBs, *i.e.*, high reactivity of Li, dendrite growth and unstable interface. Then, feasible strategies and the state-of-the-art progress towards these issues are addressed, which we focus on the modifications of battery components (separator, electrolyte and anode), and control of external conditions (charging modes, current density and service temperature). Finally, future perspectives and design strategies are summarized, aiming to providing new insights for the commercial applications of high performance LMBs.

**Keywords:** Lithium metal batteries; Lithium dendrites; External conditions control; Battery components modification.

E-mail: jwang6027@ysu.edu.cn; pengqiuming@ysu.edu.cn

## 1. Introduction

Advanced energy-storage technology has promoted social development and changed human life [1, 2]. Since the emergence of the first battery made by Volta, termed “voltaic pile” in 1800, battery-related technology has gradually developed and many commercial batteries have appeared, such as lead-acid batteries, nickel-cadmium batteries, nickel metal hydride batteries, and lithium ion batteries (LIBs) [3]. Among those, LIBs are characteristic of the highest energy density, of great commercial application to both portable electrical appliances and large power facilities [4-6]. Graphite, with a theoretical capacity limited to 372 mAh/g, is prevalent material for anode in the common LIBs assemble, which boosts the research for exploring optimal anodes with higher theoretical capacity. Fig. 1a summarizes the theoretical capacity and discharge potential of anode materials in LIBs from open literature, and they are categorized into types, *i.e.*, alloy anodes, conversion anodes and intercalation anodes according to different reaction mechanisms. Each anode materials exhibit advantages and disadvantages; however, none of them outperforms the commercial graphite counterparts [7, 8].

Li metal is considered as the “holy grail” of the anode of LIBs, given the features of: (i) the lowest electrochemical potential (-3.04 V *vs.* the standard hydrogen electrode), which enables high operating voltage, and (ii) remarkably high theoretical capacity (3860 mA/g), ten times higher than that of graphite [6, 9]. Fig. 1b depicts energy density and specific energy of a number of representative battery systems. It is convinced that, the ones containing Li anode, such as LMBs, Li-S and Li-air batteries, have an extremely high energy density, which thus attracts great research attention towards the next-generation of energy storage technology [10-12].

However, the high chemical activity of Li causes severe side-reactions in a large number of electrolytes, resulting in the formation of a thick solid electrolyte interphase (SEI) on the

surface of metallic Li. Moreover, the infinite volume expansion of Li destroys the SEI film during the electroplating process [13]. Subsequently, “dead Li” is produced by stripping of Li in dendrite roots, which leads to a low Coulombic efficiency (CE) and capacity fading [14]. After continuous cycling, the surface of Li anode is covered with dendrites and the matrix develops into a loose structure. Eventually, dendrites penetrate into the separator to cause battery failure (Fig. 1c) [6, 15, 16].

Herein, we review the challenges and progresses on LMBs. In Section 2, the challenges and progresses on Li electrodes-chemical reactivity of Li, dendrite growth and unstable interface are presented. In Section 3, we summarize the proposed strategies on anode modification, such as host (carbon, metal, and polymer) and surface modification. In Section 4, we introduce optimization of electrolytes, including liquid electrolytes and solid electrolytes. In Section 5, the possible separator modifications for inhibition of Li dendrites are discussed. In Section 6, some external conditions, relative to current and temperature, are addressed (Fig. 2). Finally, future research directions of LMBs are summarized and prospected.

## **2. Recent progresses and challenges of high-performance LMBs**

### **2.1. High reactivity of Li metal**

Atomic Li has three electrons which are populated in K and L-shell, respectively. Due to the super stability of the helium-type double-electron shell, Li atoms are highly reactive to provide the outer electron and transform readily into a stable state, *i.e.*, Li<sup>+</sup> ions [17], and it is likely to react with the other materials to generate Li<sub>2</sub>O, Li<sub>3</sub>N, Li<sub>2</sub>CO<sub>3</sub>, *etc.* [18]. As a result, Li is susceptible to reaction with various electrolytes to form thermodynamically unstable substances during battery cycling, such as, Li<sub>2</sub>O and LiF [19, 20]. These insoluble substances deposited on the surface of Li repeatedly broken and regenerated with the volume change of Li, and constitute unstable and non-dense SEI membranes [21], resulting in the consumption

of Li and decrease of CE, which ultimately causes the consequence of battery failure.

The current endeavor to overcome the high chemical activity is devoted to three aspects: First, Li alloys (e.g. LiMg, LiIn, LiSn, LiSi, LiAl), instead of the highly reactive Li metals, are applied, which reduce the reactivity of the anode [22-25]. Yet, the advantage of the extremely high capacity of Li metal is lost since the capacity drops greatly for the composite electrode. Second, a more straightforward way is to utilize passivation of Li metal surface, such as coating fluoride, Li compounds, and organic polymer which inhibits serious reactions between electrolytes and Li and thus prevents excessive loss of Li, maintaining a stable interface [26-28]. Third, the addition of film-forming additives in electrolytes, can prevent electrolytes from contacting Li, and inhibit the side reaction between electrolyte and Li from continuing to occur [29].

## 2.2. Li dendrite growth

Dendrite growth is the most severe obstacle in the safety of LMBs. At present, dendrite formation and early dendrite growth are mainly predicted through space charge, deposition and dissolution, heterogeneous nucleation and stress-driven models [30-33]. Among them, the space charge model has been widely accepted, which simply simulates the metal deposition process and can be described using the following formula:

$$\frac{\partial C_c}{\partial t} = D_c \Delta C_c - \mu_c \mathbf{E} \cdot \nabla C_c - \mu_c C_c \nabla \cdot \mathbf{E} \quad (1)$$

$$\frac{\partial C_a}{\partial t} = D_a \Delta C_a + \mu_a \mathbf{E} \cdot \nabla C_a + \mu_a C_a \nabla \cdot \mathbf{E} \quad (2)$$

$$\nabla \cdot \mathbf{E} = \frac{e(z_c C_c - z_a C_a)}{\epsilon \epsilon_0} \quad (3)$$

Where  $\mu$  is the ion mobility,  $D$  is the diffusion constant,  $E$  is the electric field, and  $C$  is the concentration. Under high voltage or high current density, anion consumption occurs near the cathode, creating a space charge and resulting in concentrated space charges near the tip of Li dendrite on anode surface. It is obvious that the growth rate of Li dendrite is directly

proportion to the anion diffusion rate near cathode. When the influence of concentration gradient is introduced, the above conclusion can be optimized to obtain the following formula [15]:

$$\frac{\partial C}{\partial x}(x) = \frac{J\mu_a}{eD(\mu_a + \mu_{Li^+})} \quad (4)$$

Where  $J$  is the effective electrode current density,  $D$  is the ion diffusion coefficient,  $\mu_a$ ,  $\mu_{Li^+}$  corresponds to its ion mobility, respectively,  $L$  is the distance between the electrodes and the  $C_o$  is initial ion concentration. In general,  $L$  and  $C_o$  are constant. When different currents are applied, two conditions occur:

i. When  $dC/dx < 2C_o/L$  is at a low current density, the concentration gradient of the ions is in a stable state, and the concentration gradient of the ions at different positions has the following linear relationship:

$$-\Delta C_a \approx -\Delta C_{Li^+} \approx \frac{\mu_a}{\mu_a + \mu_{Li^+}} JL/eD \quad (5)$$

Under this condition, the potential is a constant, and theoretically no dendrite growth exists. However, when the current density is extremely low, the ion concentration is very close to  $C_o$  though not equal, and Li surface is locally uneven and partially distorted. These problems lead to a low concentration gradient, and the battery is prone to polarization. As a consequence, dendrites with different morphologies are generated.

ii. When  $dC/dx > 2C_o/L$  is at a high current density, the ion concentration near the surface of the negative electrode drops to zero at a certain moment. This is called ‘‘Sand’s time’’, as given in the following formula:

$$\tau = \pi D \left( \frac{eC_o}{2Jt_a} \right)^2 \quad (6)$$

$$t_a \approx 1 - t_{Li^+} = \frac{\mu_a}{\mu_a + \mu_{Li^+}} \quad (7)$$

In such condition, cations and anions exhibit different mobility. Local potential on the electrode surface increases rapidly and Li dendrites are formed. When dendrite nucleates and

grows up, it has a great influence on LMBs.

To inhibit the Li dendrite growth, current efforts are as follows. First, since the uniform deposition of Li is accomplished by reducing the current density on the anode surface, one of the main strategies is to construct 3D composite electrodes to disperse the current density of Li metal surface, including low-quality 3D carbon-based hosts, high conductivity metal-based hosts, and polymer hosts with strong affinity for Li [34-36]. However, one has to note that the 3D host construction seriously reduces energy density and power density of Li anode. Second, the usual constant current charging is replaced by other charging methods, such as pulse current and sinusoidal ripple current [37, 38]. These charging methods can gently adjust the initial polarization, avoid positive feedback loops, and make Li deposition more uniform. Third, the nucleation and growth direction of Li dendrite can be regulated by changing the composition and structure of the separators (such as apply functional coatings) [39]. Moreover, separator functionalization generally has little effect on the energy density of LMBs because of no significant change in the volume or the mass of the batteries.

### **2.3. Unstable interface**

During the initial charge and discharge process, highly reactive Li reacts with organic solvents to produce insoluble Li compounds, which adhere to Li surface and form a passivation layer about 20 nm thick. In 1979, Peled first named the passivation layer as SEI [40]. Fig. 3 shows that SEI membrane is composed of many different Li compounds, including inorganic compounds near Li anode side and organic compounds near electrolyte side. Generally, inorganic Li salts in SEI can quickly transfer ions, while organic components can ease the deposition and dissolution of metallic Li [41]. However, SEI membrane is a “double-edged sword” for LMBs. On the one hand, the formation of SEI membrane avoids continuous contact between Li and electrolyte, passivates highly reactive Li, and inhibits continuous decomposition of electrolyte. On the other hand, the SEI membrane is cracked by

Li dendrite, and fresh Li is exposed to electrolyte again to form a new SEI membrane [42]. This process also frequently occurs in solid electrolytes, wherein most solid electrolytes spontaneously react with Li, resulting in unstable interface. More importantly, the weak ion conductivity at the solid electrolyte/Li interface and the uneven distribution of surface stress greatly impede the applications of LMBs. Therefore, it is necessary to stabilize electrolyte interface by reducing interface resistance and regulating the composition of SEI membranes.

Therefore, the facilitation of SEI film is a promising method to alleviate the unstable interface. For example, chemical components in liquid electrolytes (solvents, additives, and salts) are combined with Li in situ to form a uniform and dense SEI film [43-45]. In addition, an artificial SEI film is coated on the surface of solid electrolytes to reduce interface resistance, filling up electrolytes cracks and maintaining interface stability [46]. However, the constructed artificial SEI film is broken and cracked under the long-term cycle of battery, causing instability problems of the interface.

### **3. Anode modification**

#### **3.1. Host modification**

As shown in Table 1, a large number of investigations have been recently devoted to design nano-functional 3D network structures[23, 27, 36, 47-55] with high electronic conductivity, which is an effective method for improving the performance of LMBs [6]. 3D host structure can suppress the Li dendrite growth in that it not only provides spatial restrictions for Li during plating/stripping process, but also has a large specific surface area to disperse the current density [49].

##### **3.1.1. 3D carbon-based host**

Carbon materials, endowed with a range of advantages including light weight, stable chemical properties, and excellent conductivity, have become the primary choice for Li-containing composite electrodes. Recently, a lithiophilic-lithiophobic gradient layer

strategy has been developed, which consists of a lithiophilic ZnO/carbon nanotube (CNT) sublayer at the bottom and a lithiophilic CNT sublayer at the top (Fig. 4a) [56]. During plating process, Li was guided to deposit preferentially at the lithiophilic bottom. With the extension of plating time, Li was deposited at the top of the CNT, achieving uniform deposition. The results showed that the symmetric cell assembled with this lithiophilic-lithiophobic gradient layer maintained a stable lifespan for over 100 h at a current density of  $10 \text{ mA cm}^{-2}$ . In addition, a composite anode was fabricated by immersing Li in carbon fiber/amine functional group (Fig. 4b) [57]. The strong interaction between Li and the surface groups on carbon fibers rendered Li preferential nucleation in the pores and cavities of carbon fibers, which constituted reversible smooth morphology. The results showed that the full cells using this Li-C composite as the anode, coupled with NMC811 ( $\text{LiNi}_{0.8}\text{Mn}_{0.1}\text{Co}_{0.1}\text{O}_2$ ) cathode, could lead to a cell-level energy density of  $380 \text{ Wh kg}^{-1}$ . Luo's group fabricated the ion and electron hybrid conductive network by incorporating  $\text{Li}_{6.4}\text{La}_3\text{Zr}_2\text{Al}_{0.2}\text{O}_{12}$  nanoparticles into the 3D carbon nanofibers [58]. Li ions tend to deposit and dissolve along modified nanofibers, entangling on the fibers until they are covered (Fig. 4c). Symmetrical cells assembling modified nanofibers exhibited an ultra-long cycle lifespan of 1000 h and with overpotential of only 80 mV at  $5 \text{ mA cm}^{-2}$  (Fig. 4d). Reduced graphene oxide (rGO) is the most comprehensively investigated materials deposition host [49]. Luo's group prepared rGO-Li composite anode through capillary diffusion of molten Li into the rGO host [34]. The rGO host with large specific surface area was flexible and highly lithiophilic, which reduces the current density and releases the bending stress during electroplating/stripping. A Li-S pouch cell assembling rGO/Li anode could run more than 100 cycles after bending to  $180^\circ$ . However, pure Li could only undergo 35 cycles due to the infiltration of local dendrites.

Comprehensively, 3D carbon-based hosts have great potential in the structural design of LMA due to their advantages of reducing local current density and limiting volume

expansion. However, some thorny issues arising from this composite structure should be carefully considered: First and foremost, the instability of mechanical properties of carbon materials after repeated plating/stripping process may be possible to lose the ability to regulate the behavior of Li ions. Second, due to the natural lithiophobic characteristics of carbon materials, the Li deposition rate is extremely limited, so it is necessary to adopt a complex process to improve the lithiophilic characteristics of carbon materials, which, however, increases the process cost. Therefore, in the structural design of the 3D carbon host, it is necessary to ensure the structural stability and reduce the cost of lithiophilic process so that it is applicable in practice.

### **3.1.2. 3D metal-based host**

Compared with the carbon-based hosts, metal-based hosts possess higher mechanical properties and higher electrical conductivity. For example, composite anode with regular structure of Li-Cu-Li array was prepared by a simple mechanical rolling and winding stacking method, which can be steadily cycled for 900 h at a surface capacity of 50 mAh cm<sup>-2</sup> [51]. Such a unique structure effectively regulates the flow and electric field of Li<sup>+</sup> ions, and guides the controlled stripping and deposition of Li. Zhang's group studied the distribution of local multiple physical fields inside the 3D host to design a conductivity-lithiophilicity gradient 3D electrode (Fig. 4e). Under the synergistic regulation of conductivity and lithiophilicity gradients, the nucleation tendency of Li metal at the bottom was better than that at the surface. 3D metal host based on this gradient to regulate Li deposition not only guided Li metal deposition away from the separator at room temperature, but also achieved ultra-high loaded Li electrode (40 mAh cm<sup>-2</sup>), which can be operated under harsh conditions such as low temperature (-15 °C) and high current density (10 mA cm<sup>-2</sup>) [35]. Massive Li alloys have been reported for Li-S, Li-O<sub>2</sub> or LMBs such as LiMg, LiSn, LiNa, and LiIn [23, 59-61]. Recently, Luo's group constructed the bulk nanostructured Li (BNL) through the alloying reaction of Li

with SiO<sub>2</sub> [24]. The fine grain size and precipitation hardening of Li in BNL improved mechanical strength and fatigue resistance, alleviated uneven stress distribution and prevented electrode pulverization. A smooth surface and integrated anode nanostructure were maintained on a BNL anode after 50 cycles. However, fractured Li and severe pulverization were detected on a Li foil. In short, although the 3D metal-based host has high electrical conductivity and super mechanical strength, it also faces several challenges: Firstly, most of the lithiophilic metal hosts are extremely expensive, which are not realistic in practical applications. Secondly, the density of the metal matrix is higher than that of Li. Excessive use of the host causes serious dropping in energy density, which loses the advantages of LMA.

### **3.1.3. 3D polymer-based host**

Polymer functional groups with strong affinity to Li are able to regulate the diffusion of Li<sup>+</sup> ions and guide the deposition of Li on electrode [62]. Moreover, the high specific surface area of the 3D porous structure of polymeric hosts can reduce current density and prolong the time of ion depletion on anode surface [63]. 3D porous poly-melamine-formaldehyde (PMF)/Li was demonstrated to be an extraordinary composite scaffold for LMAs due to the high specific surface area and abundant polar groups (amine and triazine) (Fig. 4f) [36]. Massive polar groups of the host can effectively homogenize Li-ion flux and the porous stable structure can mitigate the volume expansion. The Li-Cu half-cell assembled the composite electrode maintained CE of 94.7% and low voltage polarization after 50 cycles at a high current density of 10 mA cm<sup>-2</sup>. Wang's group fabricated a 3D porous polyethylenimine sponge (PPS) nanofiber network on top of the Cu foil to observe the morphology transformation during plating/stripping [63]. Electrodynamic surface conduction and electroosmosis within the PPS altered the concentration and current density distribution, which enabled dendritic-free electroplating/stripping of Li. The half cells assembling PPS host exhibited an ultra-long lifespan over 800 cycles with an average CE of 99.1% at 2 mA

cm<sup>-2</sup>. Briefly, 3D host structure not only inhibits dendrite but also alleviates the infinite volume expansion of anode. One concern is that the preferred deposition of Li at the separator/anode interface, commonly referred to “top growth” mode, leads to a decrease in the utilization of 3D structures and even deteriorates the Li dendrite growth. Future development focused on tackling this issue is urgent.

### **3.2. Surface modification**

Since the Li dendrite growth is generated by the inhomogeneous current density on the surface and the non-uniform distribution of Li ions [64], surface modification is the simplest strategy to generate stable SEI film *in situ* between Li anode and electrolyte [65]. A dense and complete coating on the surface of Li-metal anode can efficiently guide the deposition of Li ions. Moreover, the protective coating can greatly inhibit the reaction between the electrolyte components and Li anodes, thus alleviating the irreversible capacity of Li metal batteries.

#### **3.2.1. Artificial film on Li surface**

A stable electrolyte/Li interface is crucial to maintain the safety of LMBs. However, active Li reacts with electrolytes to form an extremely unstable SEI membrane, whose low Young’s modulus cannot prevent the penetration of dendrites. As shown in Fig. 5a, interface modification of Li is the most widely-used method for LMBs [66]. For instance, the functional groups of 2D-MXene promoted the formation of LiF-rich SEI film at interface, which uniformly guide the flow of Li<sup>+</sup> ions and reduce the differences in Li<sup>+</sup> ion concentration on the surface (Fig. 5b) [53]. In terms of film thickness, the thickness of artificial SEI films or coating depends on the synthesis methods (Fig. 5c) [65]. For example, atomic layer deposition technology (ALD) or molecular layer deposition technology (MLD) usually produce thinner coatings, ranging from several nanometers to hundreds of nanometers. By contrast, the magnetron sputtering, spin coating and casting generate submicron to several micron thick coatings. Further, chemical reactions of Li with gas or solution can also produce dense

submicron to micron scale coatings.

However, the traditional “weak” organic membranes are difficult to maintain integrity under the attack of Li dendrite while the “tough” inorganic membranes cannot adapt to the drastic volume change of Li anode in the cycle process. Currently, Guo’s group synthesized a flexible Li polyacrylic acid (LiPAA) artificial SEI membrane [64]. Due to the high elasticity and stability of the LiPAA polymer, the flexible SEI could adapt to the deformation of Li metal during electroplating/stripping by adaptive interface adjustment, thereby reducing the occurrence of side reactions and inhibiting Li dendrite growth. Meanwhile, the LiPAA interface layer could isolate the reaction between Li and air, effectively improving the safety of LMA. In addition, garnet-type electrolyte with  $\text{NH}_4\text{F}$  is used to generate LiF layer, which not only increased stability but also prevented dendrite generation [67]. Moreover, the artificial SEI film composed of LiF had a high electron tunneling barrier and a low  $\text{Li}^+$  surface diffusion barrier, which could achieve dendrite-free plating/stripping at a high critical current density of  $1.4 \text{ mA cm}^{-2}$ .

In brief, the interface instability is primarily solved by building a strongly artificial SEI film. Moreover, artificial SEI film is a convenient and economical strategy that can be widely applied in future practical applications. However, the micro mechanism of the influence of artificial SEI films on battery performance is not completely clear, and the mechanical stability of SEI films is still beyond satisfaction after long period plating/stripping process.

### **3.2.2. Lithiophilic coating on current collector**

Traditional Cu current collector has inferior wettability with Li, which leads to non-uniform Li deposition on its surface. Fig. 5d is a schematic modification of Cu foil with capsules made of  $\text{NaMg}(\text{Mn})\text{F}_3@\text{C}$  core@shell microstructures [68]. The internal  $\text{NaMg}(\text{Mn})\text{F}_3$  core gradually released F ions and metal ions into the electrolyte to *in-situ* form a stable metal layer and a unique LiF-rich double-layer structure. The outer carbon shell

effectively reduces dissolution rate of the core, benefiting long-term stability. The battery assembled with such anode can maintain a high CE of 98% after 1000 cycles at 2 mA cm<sup>-2</sup>. With the development of cryo-electron microscopy, Li, which is sensitive to electron beam, can be observed in electron microscopy. It is discovered that Li preferentially grows along the <111> plane, which easily leads to the formation of dendrites [69]. In turn, the natural eggshell membrane (ESM) treated with trifluoroethanol (TFEA) could adjust the direction of Li growth, which greatly inhibits the growth of Li on <111> plane (Fig. 5e) [55]. A smooth surface was maintained on a modified anode after 20 cycles (Fig. 5f). However, fractured Li dendrites were detected on a Li foil (Fig. 5g). Symmetrical cells assembling modified anode exhibited an ultra-long cycle lifespan of 1200 h and with overpotential of only 45 mV at 5 mA cm<sup>-2</sup> (Fig. 4h).

A large number of materials can be utilized in surface modification, including metal materials, metal salts, oxides, nitride, phosphates, fluoride, and polymers. The difficulty in the application of artificial coating is to produce uniform thin layer. Traditional wet chemical synthesis is difficult to achieve uniform deposition, so ALD and MLD are more practical. These advanced processes can not only manufacture nanoscale uniform film, but also promote better performance in reversible capacity, cycle stability, rate performance and safety.

## **4. Electrolyte modification**

### **4.1. Liquid electrolyte**

Liquid electrolyte has better ionic conductivity which closely contacts with Li. But the lowest unoccupied molecular orbital (LUMO) of the electrolyte is lower than the Fermi level of Li anode, which causes Li reduction [70]. Therefore, the Li metal anode does not have a stable liquid electrolyte due to its low electronegativity. On the contrary, Li metal anode is prone to be dynamically stable when a passivation layer is formed at the interface between the Li anode and the electrolyte. Therefore, electrolyte modification which changes the

composition of the electrolyte is expected to obtain a stable passivation layer and exhibit better stability [71]. Compared with carbon-based electrolytes, ether-based electrolytes facilitate the formation of protective oligomers on SEI membranes, making them more compatible with Li [72]. Therefore, a battery equipped with an ether-based electrolyte has better stability and higher CE than those of the battery equivalents containing a carbon-based electrolyte (Fig. 6a,b) [45, 72-78].

#### **4.1.1. High concentration Li salt**

In conventional electrolytes, concentration of Li salt is 1 mol, which ensures that the electrolyte has an appropriate viscosity. It is found that high concentration electrolyte has excellent dendrite suppression and high conductivity performance which may be applied to LMBs [72, 79]. Recent studies have shown that the use of 4M LiFSI-DME as electrolyte resulted in nodule-shaped Li deposition (Fig. 6c) [45]. The increase in solvent coordination and the increase in the availability of lithium ion concentration accounted for the origin of the superior performance of 4M electrolyte. Symmetrical cells assembling 4M LiFSI-DME electrolyte exhibited an ultra-long lifespan of 6000 cycles at 10 mA cm<sup>-2</sup>. In a similar approach, the FSI ion provided by 10 M LiFSI-EC/DMC electrolyte made the interface layer with high fluorine content between Li and electrolyte, which effectively inhibited the formation of Li dendrites [80]. The results show that the Cu|Li cell assembling 10 M LiFSI-EC/DMC electrolyte could be cycled at 0.2 mA cm<sup>-2</sup> for more than 240 cycles with an average CE of 99.3%.

Comprehensively, the high concentration electrolyte exhibits great potential in the improvement of electrolyte under practical conditions, but some problems still are challenging us: (i) high concentration electrolyte significantly increases the viscosity of the electrolyte, which extends the soaking time of the battery; (ii) the cost of Li salt in commercial electrolyte accounts for about 70%, increasing the price of electrolyte; (iii) many mechanisms in the high

concentration electrolyte are still unclear, such as the electrolyte interface structure and ion transfer mechanism. Therefore, in the future research, the combination of calculation and experiment should be used to explore the novel high concentration electrolyte system and internal mechanism.

#### **4.1.2. Electrolyte additives**

Additives have different functions such as conductive additives, flame retardant additives, and film-forming additives. Recent studies have shown that the content of LiF in SEI film affects battery performance [81]. For example, an SEI composed of LiF, Sn and Sn-Li alloy was prepared by pretreatment of Li surface with an electrolyte containing SnF<sub>2</sub> [44]. This artificial SEI membrane not only used the characteristics of LiF high ionic conductivity to rapidly diffuse Li<sup>+</sup> ions, but also stored Li through Sn-Li alloy. As a result, the symmetrical cells delivered good cycling performance and maintained a long-term lifespan of 800 h at 1 mA cm<sup>-2</sup>. Recently, non-flammable electrolytes were fabricated by adding triethyl phosphate (TEP) electrolyte additives [82]. The coordination of TEP with Li<sup>+</sup> could effectively inhibit the adverse reaction of the solvent molecules to the anode, which inhibited dendrites and made the electrolyte non-flammable, improving the safety performance of battery. Consequently, the cells using the 1:2 LiFSI-TEP electrolytes remained intact during the nail penetration test, whereas the cells using the carbonate electrolyte is cracked and flamed (Fig. 6d). Stable SEI membranes could be prepared by adding vinyl ethylene carbonate (VEC) film-forming additives [29]. The SEI membranes formed in 10% VEC electrolyte contained a relatively high content of polycarbonate and massive salt decomposition products of LiPF<sub>6</sub>. Therefore, the SEI membranes were stable and smooth, which effectively prevent dendrite growth. The results showed that the VEC electrolyte was able to achieve a long-life of 100 cycles at 0.25 mA cm<sup>-2</sup> in a Li-Cu cell configuration.

Although the SEI membrane formed using electrolyte additives is relatively stable, the

dendritic penetration cannot be excluded completely, especially after the long-term cycle. In general, a combination of two or more additives, rather than single one, is used to generate synergistic effect to improve the SEI membrane stability and battery safety. But, due to the complexity of interface reactions, it is very difficult to design additives. Therefore, the strategy of additives cooperation with other methods is preferred.

#### **4.1.3. Specific solvents**

In order to improve the intrinsic safety of LMBs, flame-retardant electrolytes, such as organic phosphate electrolytes (OPEs) is able to intrinsically eliminate fire hazards. However, the poor compatibility of LMA limits the practical application of this kind of solvent. Guo's group proposed to modify OPEs by  $\text{LiNO}_3$  to form nitrated interface to improve the electrochemical incompatibility between OPEs and Li metals [83]. Benefit from the structure of the nitrating interface, the modified OPEs achieves a dendrite-free morphology, performing a high energy density battery with long cycle life and excellent safety. Ionic liquid (IL) electrolytes can guarantee the safety and high performance of LMBs, but its high viscosity and poor ion transport capability have become the bottleneck of further improvement of Li batteries. Lee's group designed a local highly concentrated IL electrolyte containing fire-retardant hydrofluoroether. The addition of 1,1,2,2-tetrafluoroethyl 2,2,3,3-tetrafluoropropyl ether (TTE) resulted in lower viscosity and better separator wettability of IL electrolyte, which was conducive to the migration of Li ions to LMA. The results showed that Li/LiCoO<sub>2</sub> full cell equipped with modified IL electrolyte had good specific capacity (89 mAh g<sup>-1</sup>) and the long cycle performance (keep the rate of about 80% after 400 cycles) [84].

Recently, acetonitrile electrolyte with a high salt concentration has been developed for the first time for LMBs [43]. This electrolyte not only had a high degree of dissociation but also had excellent intrinsic ion conductivity. This acetonitrile electrolyte enabled a stable

long-term cycling capability of the symmetric cell for over 2000 h at a high current density of  $2 \text{ mA cm}^{-2}$ . Although sulfone electrolyte has excellent oxidation stability and it is suitable for high-voltage battery systems, it has poor stability to Li, which limits its application in LMBs. Zhang's group added non-solvent fluorinated ether to sulfone-based solvent to form localized high-concentration sulfone electrolytes, which effectively solved the problems of high viscosity and poor wettability of sulfone-based electrolytes [85]. The Li/Cu cells assembling sulfone electrolytes exhibited dendrite-free morphology and superior cycling performances over 150 cycles with high CE of 98.8%.

In summary, the liquid electrolyte known as the “battery blood” is responsible for the ion transport during the battery charging and discharging process. However, due to the high intrinsic reactivity of Li, side reactions occurring between the organic liquid electrolyte and Li are inevitable, forming a fragile SEI membrane. In addition, flame retardant electrolytes are currently one of the most advanced technologies to ensure the safety of LMBs. At this point, there is still plenty of developing room to find a novel liquid electrolyte system and optimize the electrolyte ratio to meet the actual demands.

## **4.2. Solid electrolyte**

The application of solid electrolytes in LMBs is favorable based on energy density and safety considerations [86-88]. Fig. 7a summarizes the performance of some typical solid electrolytes [6]. The advantages and disadvantages of different electrolytes can be easily identified by using this radar plot, which is beneficial to the design of the electrolyte. Among them, inorganic solid electrolyte suffers from chemical instability. However, the poor ion conductivity of the polymer electrolyte at ambient temperature, which is one order of magnitude lower than that of sulfide-based inorganic solid electrolyte, is the main factor hampering its practical application (Fig. 7b) [89-101].

### 4.2.1 Inorganic solid electrolyte

Inorganic solid electrolyte mainly refers to the general term of inorganic  $\text{Li}^+$  ion conductive materials such as oxide [67, 89, 102], nitride [90], sulfide [91-93], borate [94], and phosphate [103]. This type of solid electrolyte has a convenient manufacturing process and a wide operating temperature range (50 to 200 °C). Recent reports demonstrated that the inert  $\text{Li}_2\text{CO}_3$  layer on the surface of garnet-type solid electrolyte reduced electrolyte conductivity and increases impedance at the interface [104, 105]. An amorphous  $\text{Li}_3\text{PO}_4$  layer was constructed on  $\text{Li}_{6.5}\text{La}_3\text{Zr}_{1.5}\text{Ta}_{0.5}\text{O}_{12}$  (LLZTO) by ALD technology, which improved interface conductivity and filled cracks on the surface of LLZTO electrolyte, thus the electrolyte performs better contact with Li (Fig. 7c) [46]. The results showed that the symmetrical cells assembling modified LLZTO exhibited an ultra-long cycle lifespan of 140 h and with overpotential of only 16 mV at 0.2 mA  $\text{cm}^{-2}$ . The interfacial charge transfer resistance between a Li metal anode and an inorganic electrolyte is of key interest to assess the rate capability of future all-solid-state batteries. Doping elements into the inorganic electrolyte to stabilize the  $\text{Li}^+$  conductive cubic phase is a promising scheme for reducing interfacial charge transfer resistance. Among them, Ta, Nb, and Al are the most common dopants, which cause the reduction of Zr to a certain extent, following the order of Ta < Nb < Al [106].

To some extent, the ionic conductivity of inorganic solid electrolyte has been encountered a bottleneck, wherein. The interface compatibility between inorganic electrolyte and electrode is challenging.

### 4.2.2. Polymer solid electrolyte

Polymer solid electrolytes are superior to inorganic solid electrolytes in film-forming aspects [107]. Unfortunately, poor oxidation resistance and low ionic conductivity seriously hinder its practical application. In order to ameliorate the disadvantages of weak ionic conductivity and low Young's modulus, it is necessary to add other chemicals to improve

performance [95]. For instance, MXene surface functional groups were used to transfer Li<sup>+</sup> ions in the poly(propylene oxide) elastomer (ePPO) through Lewis acid reaction, thereby obtaining high ion conductivity of  $4.6 \times 10^{-4} \text{ S cm}^{-1}$  and high Young's modulus of 10.5 MPa [96]. The results showed that the Li/MXene-ePPO/Li cell could run more than 500 h. By contrast, Li/ePPO/Li cell only undergoes 200 h due to the interfacial resistance increasing. Recently, polymer electrolyte with flame retardant properties had been developed, including 10  $\mu\text{m}$  thick porous PI polymer layers as supporting material, decabromodiphenyl ethane (DBDPE) as flame retardant, and PEO+LiTFSI as polymer ionic conductor (Fig. 7d) [108]. This composite structure could be roasted under a flame for 24 s. Moreover, the LiFePO<sub>4</sub>/Li half cells assembling this non-flame polymer electrolyte showed a long-term lifespan of 300 cycles at 0.5 C and a high rate performance of 131 mAh g<sup>-1</sup> at 1 C. Gel polymer electrolyte (GPE) composed of a polymer matrix and liquid solution has good elasticity, ion conductivity, and compatible with Li [109]. A hierarchical gel electrolyte structure is proposed via in situ gelation of an organic solvent supported on functionally-modified SiO<sub>2</sub> nanoparticles [97]. The synergistic effect of SiO<sub>2</sub>-GPE film provided a highly compatible electrode/electrolyte interface and effectively inhibited Li dendritic growth. The LiFePO<sub>4</sub>/SiO<sub>2</sub>-GPE/Li cells exhibited a long life span of 700 cycles (at 1 C rate) and relatively high capacity retention of 88.42 %.

The limitation of solid polymer electrolytes lies in low ion conductivity and poor mechanical strength limit their practical applications. Therefore, it is necessary to strengthen the study in the relationship between structure and ion transport, ion transport kinetics, interfacial compatibility and stability. Exploration of new research and characterization methods of amorphous solid polymer electrolytes is necessary, which in turn can guide the design, screening and preparation of polymer chains.

### 4.2.3. Composite solid electrolyte

Inorganic/organic composite solid electrolytes have drawn attention because they can overcome defects by combining the advantages of inorganic solid electrolytes and organic solid electrolytes [98, 110]. Cui's group incorporated garnet-type  $\text{Li}_{6.4}\text{La}_3\text{Zr}_2\text{Al}_{0.2}\text{O}_{12}$  (LLZO) network into a PEO polymer matrix to obtain a hybrid LLZO-PEO electrolyte [100]. In this structure, LLZO enabled with high ion conductivity, which allowed  $\text{Li}^+$  ions to migrate quickly, and the polymer matrix provided excellent mechanical flexibility (Fig. 7e). The composite solid electrolyte could effectively suppress the dendrite growth for 500 h at a current density of  $0.2 \text{ mA cm}^{-2}$  in a symmetric cell. In addition, nonflammable polyvinylidene fluoride-hexafluoropropylene copolymer (PVDF-HFP) is usually applied as a substrate of gel polymer due to its excellent affinity with liquid electrolyte, but poor ionic conductivity makes battery unable to work normally [111]. Therefore, Wen's group used  $\text{Li}_{6.4}\text{Ga}_{0.2}\text{La}_3\text{Zr}_2\text{O}_{12}$  to coordinate with TEP to form a Lewis base to act on PVDF-HEP, which in turn allowed PVDF-HEP chain to be defluorinated and cross-linked to improve ionic conductivity [101]. As a result, the full cells assembling the modified electrolyte exhibited a long lifespan of 360 at 0.5 C with an average CE higher than 98%.

In summary, solid electrolyte is considered to be the "holy grail" of solving the safety problem of Li metal batteries. Typically, inorganic/organic solid electrolyte is expected to be an electrolyte with high ionic conductivity and mechanical flexibility, but the poor compatibility between inorganic and organic interfaces limits the stability of the battery's long cycle. Therefore, future improvement in the direction is emphasized on the design of the arrangement of inorganic materials, development of novel synthetic routes and reducing the size of inorganic electrolyte, with the aim to enhance the compatibility of inorganic materials.

## 5. Separator modification

## 5.1. Inhibit dendrite growth

Separator is an extremely significant part of battery, which is related to cost and safety performance [112, 113]. Currently, commercial separators are only physical separation devices with high ionic conductivity, but they do not possess the function of inhibiting dendritic growth. Therefore, it is essential to design functionalized separators for the application of LMBs. Among them, loading a coating on the separator to regulate the uniform nucleation of  $\text{Li}^+$  ion deposition has obvious advantages, because it can prevent the Li dendrite growth in the first place, rather than trying to deal with the after effects [39].

### 5.1.1. Change in direction of dendrite growth

Eliminating the dendrites before them touching the separator prevents the cell from short-circuiting. A strategy to change the direction of dendrites growth was recently reported by coating separator with functionalized carbon nanoparticles (FNC) [39]. During the cycling process, dendrites grow from FNC layer and anode at the same time to each other until they come into contact (Fig. 8a). Eventually, Li deposition transforms from low-dimensional Li dendrites to high-dimensional dense Li layers. Li/LiFePO<sub>4</sub> coin cells with FNC modified separator could operate for more than 819 cycles and maintain a dendritic-free morphology, while only 216 cycles were possible for commercial separator due to the local dendrite penetration (Fig. 8b, c). In addition, ultra-thin Cu film coated on separator could effectively promote the electrochemical transfer of Li and reduce the accumulation of “dead Li” [114]. When Li deposited on the surface of separator and collector contacts with each other, the growth direction is different, and subsequent Li growth occurred in the horizontal direction, thereby inhibiting the vertical growth of Li dendrites via the separator. The results showed that the Li/Cu half-cell assembling modified separator enabled a long stable cycle life (300 cycles with 95.6% CE), while the control cell achieved an average CE value of 90.1% until 250 cycles.

### **5.1.2. Improve ionic conductivity of separator**

Improving ionic conductivity of separator contributes to rapid transfer of  $\text{Li}^+$  ions in battery, which is also positive in inhibiting dendrites growth. Recently, a composite separator was fabricated by using Si-polyacrylic acid (Si-PPA) to form a Li/Si alloy-LiPAA layer under induction of electrolyte [115]. This layer was an excellent  $\text{Li}^+$  ion conductor, which improves  $\text{Li}^+$  ion conductivity of separator, and thus suppresses the growth of dendrites. The Li-Li cells assembling composite separator showed a low overpotential of 25 mV at  $0.5 \text{ mA cm}^{-2}$  over 1000 h and a long lifespan of 600 h even at high current densities of  $1 \text{ mA cm}^{-2}$ . Additionally, coating water-borne nano-sized molecular sieve with polyethylene (PE) separator significantly improved the conductivity of  $\text{Li}^+$  ions due to specific pore structure and channel environment [116]. Therefore, the capacity retention rate of LMBs equipped with the composite separator was 19.5% higher than that of the original PE separator after 100 cycles. Modification of the separator was performed by combining with a strong adhesion polydopamine (PDA) [117]. The study elucidated that the ionic conductivity of the separator was remarkable enhanced (from  $0.36 \text{ mS cm}^{-1}$  to  $0.45 \text{ mS cm}^{-1}$ ), and the capacity retentions of the battery was significantly improved (from 78 % to 83.4 %). In addition, researchers developed various types of coatings to enhance ionic conductivity, such as ceramic materials, metal-organic frameworks (MOFs), and composite layer [118-121]. These coatings play the roles of guiding uniform transmission of  $\text{Li}^+$  ions, adjusting deposition form of Li, and reducing the polarization of the battery.

### **5.2. Prevent dendrite penetration**

The separator is the last defense against Li dendrites. Therefore, it is extremely important to increase the mechanical strength of the separator to prevent the dendrite penetration and to load the short circuit warning system in the separator. In addition, monitoring Li dendrite growth is the most intuitive strategy to prevent LMB short circuit. If the contact of the interior

of the separator with the Li dendrite tip is directly observed in the detector, the short circuit of LMB can be completely avoided [122].

### **5.2.1. Increase mechanical strength of separator**

When separator modulus exceeds dendrite modulus, separator can effectively prevent dendrite puncture. It has been calculated that when shear modulus of separator is twice that of Li dendrites, separator can effectively inhibit dendrite penetration [123]. A shear modulus as large as 6.7 GPa is revealed for the ultra-strong poly(p-phenylenebenzobisoxazole) nano-fibers separator prepared from Zylon fibers [124] which is close to the theoretical value of inhibiting Li dendrites, and thus the battery assembled with this separator performs surprising inhibitory effect on Li dendrites in practical applications. Inspired by the idea that shield surface bending can effectively resist spear penetration, nano-shield separator was designed to prevent dendrite penetration by spinning SiO<sub>2</sub> nanospheres on commercial polyolefin separators [125]. Mechanical stress calculation revealed that nano-shield separator could reduce stress when separator faced dendrite penetration. More importantly, the stress of the separator was minimal when the curvature of the shielding separator was equal to the curvature of the dendrite tip (Fig. 8d). In addition, excellent physical and chemical stability of SiO<sub>2</sub> not only suppressed dendrites but also enhanced the wettability between electrolyte and separator. The results showed that the Li-plating lifespan of Li/Li symmetrical cell could reach more than 110 h, which was one of the longest cycle lifespan of LMA and 5 times longer than that of blank separator.

### **5.2.2. Monitor dendrite growth**

In fully encapsulated battery, it is difficult to predict whether dendrites have penetrated separator without dismantling battery. To solve this problem, PE/Cu/PE composite structure separator was designed for early monitoring of Li dendrites [122]. This Cu metal layer was connected to anode, resulting in a potential difference from Cu layer to anode. The the

potential difference became zero when Li dendrite punctured the separator (Fig. 8e). Therefore, composite separator could determine the growth of dendrites by monitoring whether potential difference was zero, and avoid short circuits caused by Li dendrites. In another experiment, the significant variation in voltage was caused by the accumulation of electrons at the interface between Li dendrites and red phosphorous (RP), when they are contact with each other [126]. Therefore, the Li dendrite grows in the cell could be monitored only by observing the external voltage change.

Comprehensively, in the design criteria of the new separator, it is aware that the separator acts as a barrier in-between positive and negative contact and the mechanical strength has to be high enough to limit the Li dendrite growth. Moreover, it is necessary to explore functional separators in regulating ion conduction, stabilizing positive and negative active substances, and detecting battery short circuits.

## **6. Improving LMB performances through external modification**

In the case of external modification, the improvement of LMB performances is mostly involved two aspects: current management and temperature control.

### **6.1. Current management**

Lorentz force and external power source significantly affect the surface charge distribution of Li [127]. Therefore, it is very important to regulate growth rate and growth mode of Li through charging mode and current density. On the one hand, pulse charging has been confirmed effective to uniform ion concentration between electrodes in LIBs [128, 129]. Moreover, Li dendrite growth in a pulse charging mode revealed competitive relationship between  $\text{Li}^+$  ion diffusion time scale and the reduction of Li/SEI interface, and proved that Li dendrite growth could be remarkably inhibited by appropriate pulse frequency [130]. Both theoretical and experimental results proved that the service life of LMBs could be greatly extended by optimizing pulse current [37]. Molecular simulation results showed that the loose

structure between cations and anions can increase the transport of Li<sup>+</sup> ions, and eventually stabilize the deposition of Li. As a result, the Li symmetric cells could reach more than 48 cycles under pulse current cycle conditions, which was 2.4 times higher than that of constant current cycle. Under sinusoidal ripple current charging condition, the relaxation period promoted more uniform Li deposition, and resulted in a smooth and dense granular appearance of Li deposition (Fig. 9a,b) [38]. In addition, when the cells were charged with square wave current, the deposition of Li led to a mossy morphology, reducing the amount of Li dendrites (Fig. 9c). However, the dendrite growth of Li was observed under constant current charging, (Fig. 9d). Therefore, the cycling performance of sinusoidal ripple current charging (250 cycles) was considerably improved compared to square wave current (163 cycles) and constant current (26 cycles) charging (Fig. 9e).

On the other hand, the effects of current density on the surface morphology of Li powder electrode have been systematically reported, and an empirical formula has been established [131]:

$$Q = \frac{5.58133}{(1 - 1.0286J + 0.4957J^2)} \quad (8)$$

$$((J - 1)^2 + 1) Q \approx 11 \quad (9)$$

Where  $J$  is the current density and  $Q$  is the total amount of charge.

The result indicates that when the current density is less than 1 mA cm<sup>-2</sup>, dendrites are not easily formed [131]. However, a larger current density does not invariably promote the generation of larger dendrites, because more Li deposition sites were generated in the case of a high current density, resulting in a dendrite-free state. For example, under a higher current density condition, the migration of Li on the surface extensively accelerates, eliminating dendrites and constituting a dense layer structure (Fig. 9f). [132] Therefore, the battery after high current healing of Li dendrites still maintained 98% high CE after 250 cycles at ~0.75 mA cm<sup>-2</sup> (Fig. 9g). This trend has also been confirmed by recent simulations, in which Li

electrochemical reaction barrier was smaller than Li diffusion barrier, and then the high self-heating current could slow down the generation of dendrites [133].

## 6.2. Temperature control

Temperature plays an important role on LMBs by varying the thickness of SEI membrane, the morphology of dendrites, and the onset time of dendrites. It was recently reported that the occurrence time of dendrites and the thickness of SEI film increased monotonically with increasing temperature (Fig. 10a,b) [134]. The evolution of dendrites in ether-based electrolyte at -80 °C and the morphological changes of SEI membranes [135] showed that the nucleation overpotential of Li was continued to increase as the temperature was decreased, resulting in a smaller critical nucleation size. In addition, the nucleation size of Li was increased and the deposition density of Li was enhanced when the temperature increased from room temperature to 60 °C (Fig. 10c) [136]. The Li symmetric cells could reach more than 150 h at 60 °C, which was more than 2 times than that at 20 °C. Characteristics based on cryo-electron microscopy observations reveal that SEI film at a high temperature of 60 °C had a unique structure [137], wherein the innermost layer was an amorphous polymer matrix, and the external interface near organic electrolyte was crystalline  $\text{Li}_2\text{O}$  (Fig. 10d). This special SEI film structure provided high mechanical stability during charging and discharging process, which in turn improved CE and battery lifespan.

Basically, a higher temperature leads to a lower over-potential, resulting in a larger nucleation radius and a lower nucleation density, which reduces dendrite formation. On the contrary, a lower temperature is more likely to cause the dendrite formation. Note that the battery cycling inevitably generates heat, which can greatly increase the internal temperature of the battery. Therefore, it is valuable to reduce dendrite growth by using the heat generated inside the battery. Moreover, future researches based on thermodynamic parameters should be included: dendrite growth, Li stripping, advanced non-flammable electrolytes *etc.*

## 7. Conclusions and outlooks

A low energy density of LIBs is a bottleneck, which is far behind a critical level of 500 Wh/kg. However, a promising candidate of LMBs still has serious problems to be resolved, which can be summarized as follows: the high chemical activity of Li, uncontrollable growth of Li dendrites, and unstable interfaces. More seriously, these problems are interrelated. Only when all of them are solved well in future, the commercialization of LMBs can be realized. Aimed at these issues, we outline several main research directions for LMBs:

1. Cyclability at a high current density. A majority of reported LMBs were tested at a low current density in button batteries. Moreover, the designed batteries produced a large amount of “dead Li” after a high current density cycle, resulting in extremely low Coulombic efficiency, and making battery unable to continue working after dozens of cycles. These data can not provide some accurate parameters for the design of commercial batteries.

2. A thickness of Li foil electrode. The commercial Li battery with a high energy density requires Li foil thickness of  $\sim 50$   $\mu\text{m}$ . However, the infinite volume expansion of LMBs in the charging and discharging process has not been well solved. Thus, it is difficult to reduce the thickness of Li foil to commercial level at present.

3. Mechanisms of Li dendrite growth. The generation of Li dendrites is mostly observed by *ex-situ* scanning electron microscopy, which might damage original properties and lead to some misleading results. Thus, it is desirable to observe the Li dendrite growth under *in-situ* transmission electron microscopy, which will clarify the mechanisms of Li dendrite.

4. Solid electrolytes. Solid electrolytes are considered to be the “holy grail” for solving safety problems of LMBs, especially inorganic-organic composite solid electrolytes. However, the poor compatibility of composite solid electrolytes in relative to interface problem has not been well solved. The large interface resistance and interface fluctuations need to be further investigated in detail.

5. SEI membrane on anode. SEI membrane not only regulates the transfer of  $\text{Li}^+$  ions from electrolyte to electrode, but also accounts for irreversible capacity loss. Understanding the properties of SEI membrane is crucial to stabilize LMBs cycle and increase energy density. Nowadays, with the rapid development of cryogenic transmission electron microscope, SEI membranes that are sensitive to electron beams and air can be well characterized, which provides enormous support for the further composition/mechanism analysis of SEI membranes.

6. Separator modification. The coatings on polymer separator can effectively inhibit dendrite growth. Also, the separator derived from solid electrolyte can simultaneously regulate the deposition of Li ions and prevent dendrite growth. However, the modifying of polymer separator usually sacrifices separator flexibility, which makes it impossible to apply to emerging wearable devices.

7. LMBs safety. Owing to the presence of flammable organic electrolytes and highly active Li, the safety issue has always been concerned. The subjects on the stable Li electrode and non-flammable electrolyte and/or stable substrates are extremely attractive directions.

With the rapid development of fundamentals, characterization techniques, and materials science, we believe, the problems will be well solved in LMBs, although which cover multi-disciplinary issues. The commercial applications of LMBs are no longer far away.

### **Declaration of Competing Interest**

The authors declare that they have no known competing financial interests or personal relationships that could have appeared to influence the work reported in this paper.

### **Acknowledgements**

We greatly acknowledge the financial support from National Natural Science Foundation-Outstanding Youth Foundation (51771162, 51971194) and Hebei Province Talent

project (A201910002). We would like to express our gratitude to Ministry of Education Yangtze River scholar professor Program.

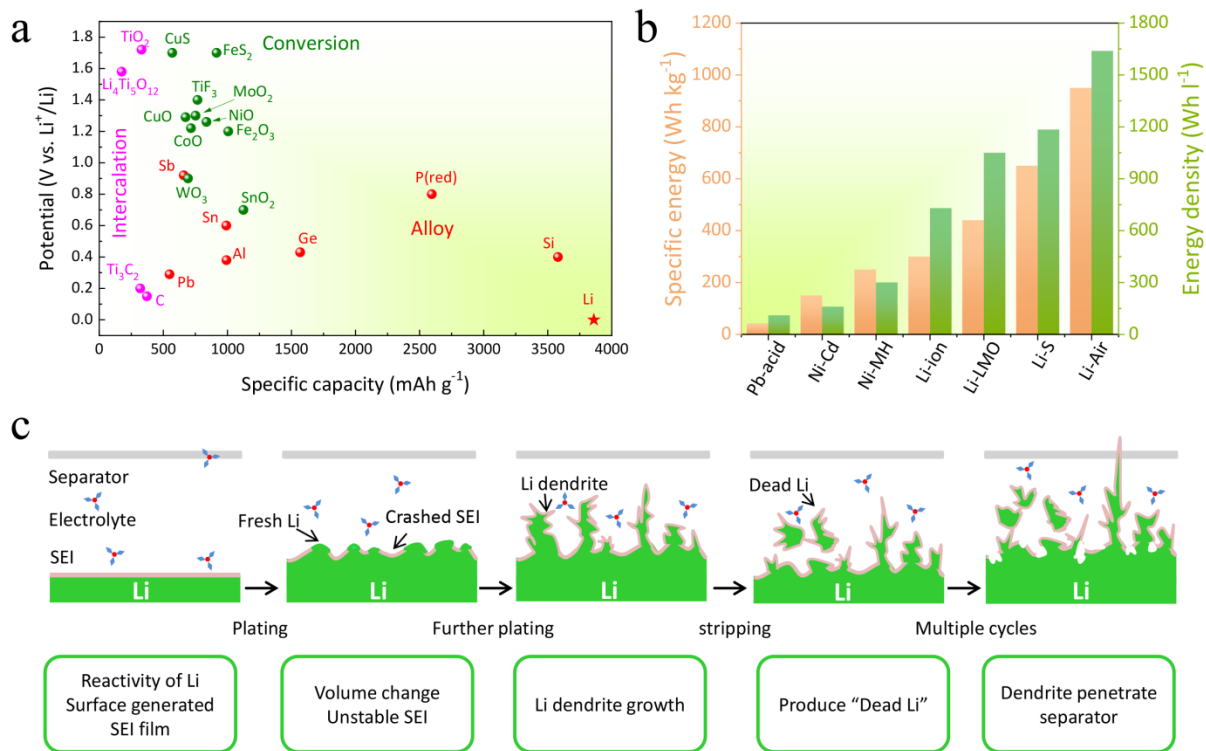


**Fig. 1.** (a) Theoretical specific capacity and discharge potential of representative Li battery anodes. (b) Achievable energy density and specific energy of various battery systems at present. (c) Schematic of LMBs plating/stripping process.

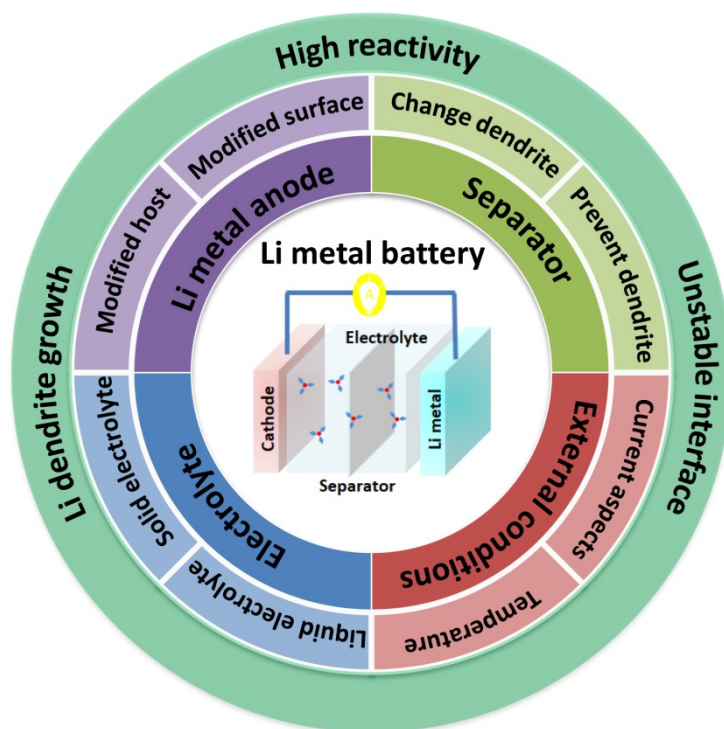


**Fig. 2.** Schematic illustration of the challenges and solutions in relative to LMBs.

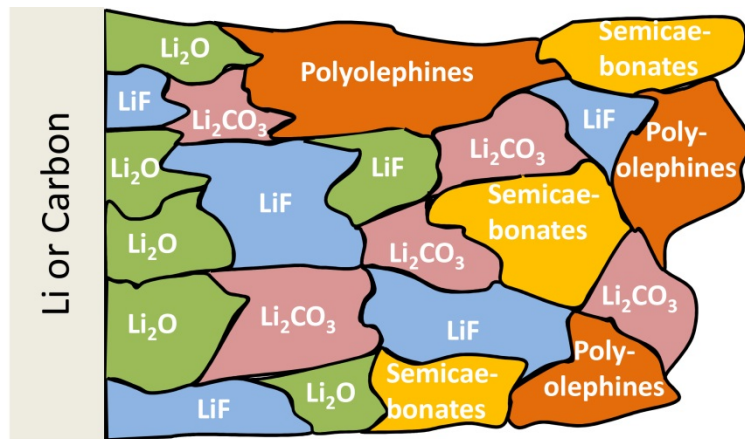


**Fig. 3.** Schematic diagram of the multiphase SEI structure.

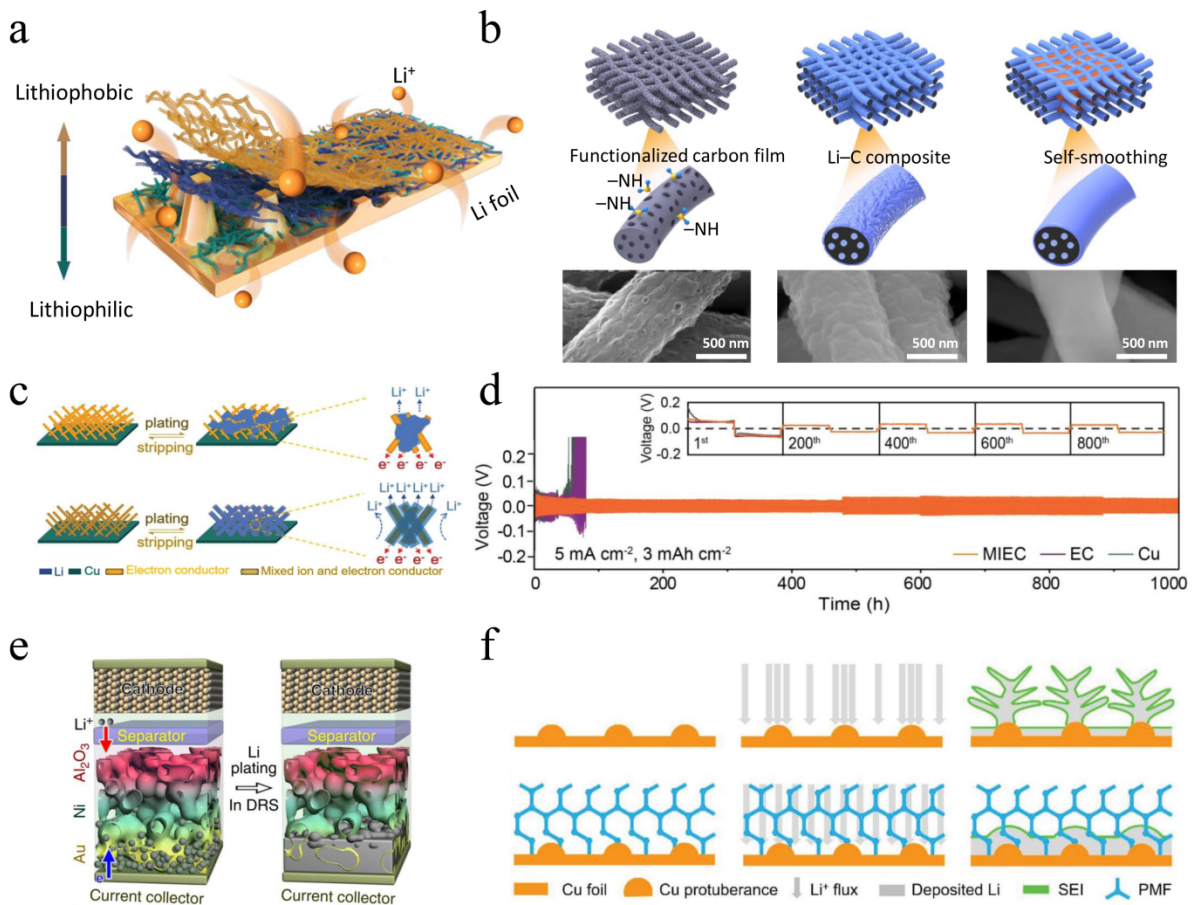


**Fig. 4.** (a) Schematic of 3D carbon nanotubes with lithiophilicity gradient [56]. Copyright 2018, Springer Nature. (b) Self-smoothing Li-C anode supported by amine-functionalized 3D mesoporous carbon fibers [57]. Copyright 2019, Springer Nature. (c) Schematic of homogeneous Li plating along Li<sub>6.4</sub>La<sub>3</sub>Zr<sub>2</sub>Al<sub>0.2</sub>O<sub>12</sub> modified carbon nanofibers. (d) Long-term cycling performance of symmetric cells with Li<sub>6.4</sub>La<sub>3</sub>Zr<sub>2</sub>Al<sub>0.2</sub>O<sub>12</sub> modified carbon nanofibers as anode scaffolds [58]. Copyright 2018, Wiley. (e) Schematic of the deposition of Li in a 3D porous Ni scaffold with conductivity/lithiophilicity gradient [35]. Copyright 2019, Springer Nature. (f) Li is deposited directly or through PMF on Cu foil [36]. Copyright 2018, Wiley.

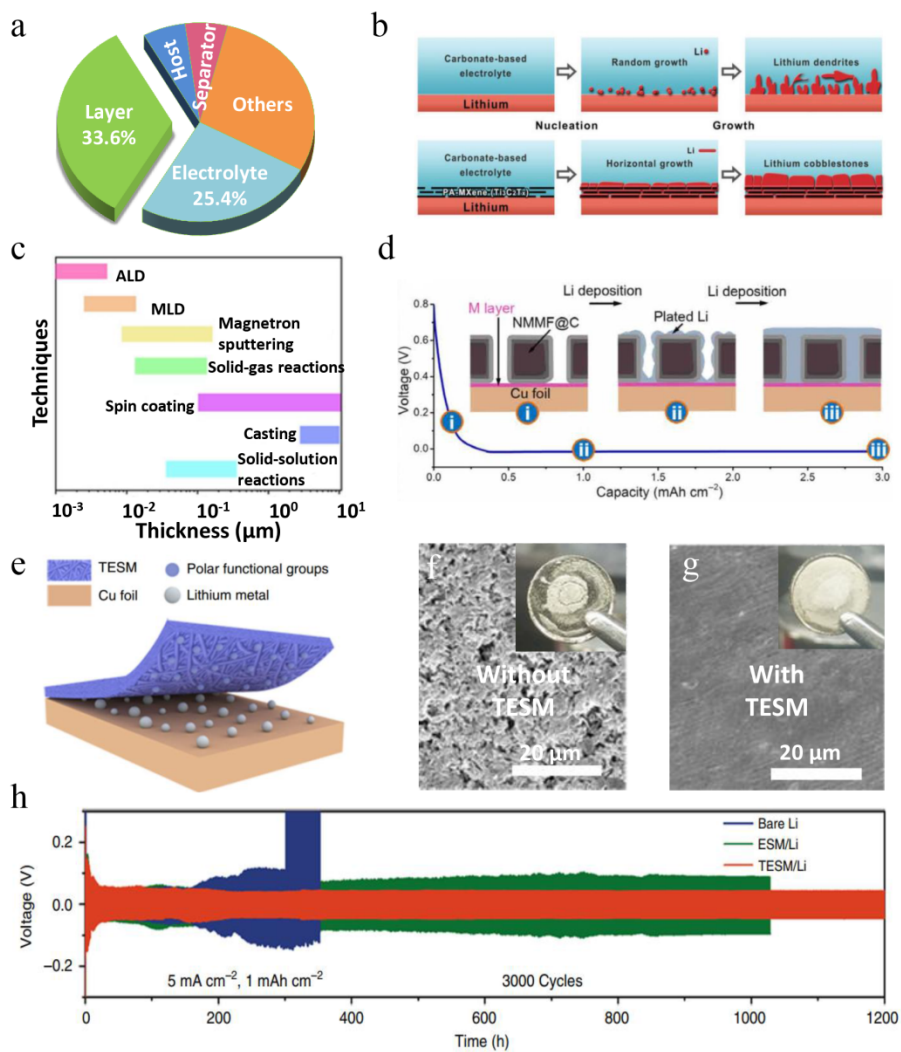


**Fig. 5.** (a) Schematic of the number of papers on different modification methods of LMBs from 1941 to 2019 [66]. Copyright 2020, Wiley. (b) Schematic of Li deposited on anode with or without MXene layer on the surface [53]. Copyright 2019, Wiley. (c) Coating thickness range obtained by various coating strategies [65]. Copyright 2020, Elsevier. (d) The staged discharge curve of the NMMF@C-Cu anode and the corresponding schematic of Li electroplating processes on NMMF@C-Cu [68]. Copyright 2020, National Academy of Sciences. (e) Schematic of Li growth on TESM-modified Cu foil; (f-g) SEM morphology of Li deposited on Cu foil without and with TESM modification. The insets show actual image of the corresponding Li foil. (h) Symmetric cell cycling performance of TESM at a current density of  $5 \text{ mA cm}^{-2}$  under a deposition capacity of  $1 \text{ mAh cm}^{-2}$  [55]. Copyright 2020, Springer Nature.

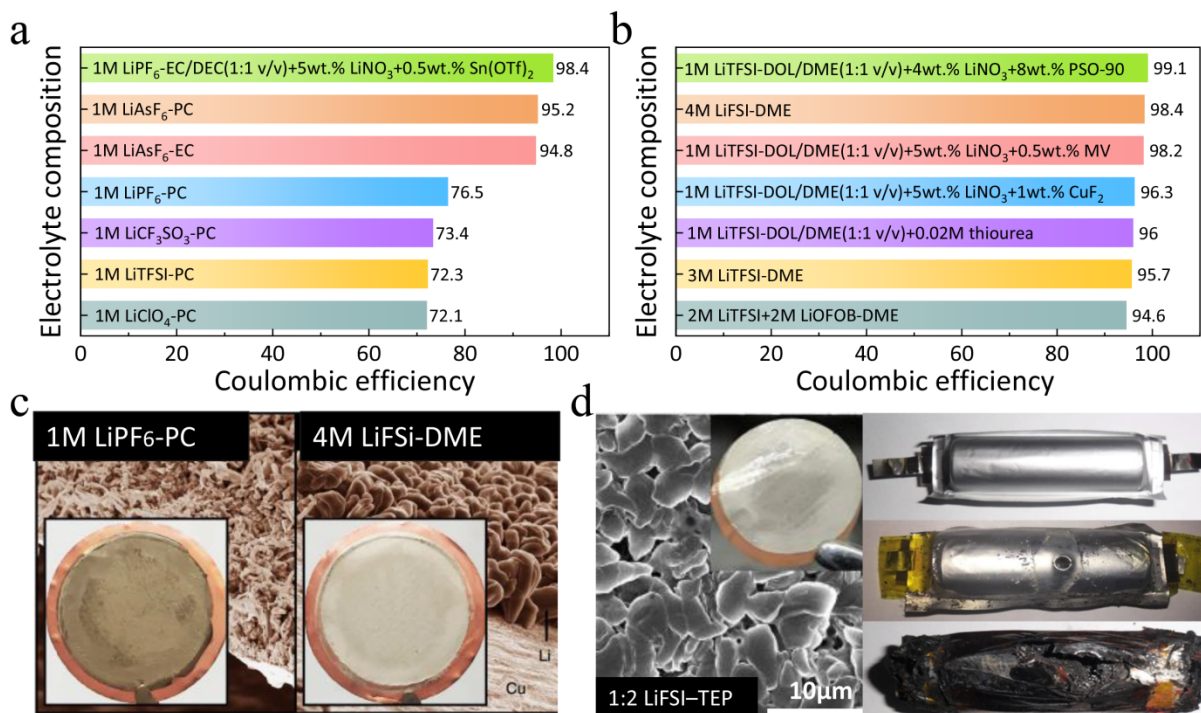


**Fig. 6.** (a) Coulombic efficiency of Li-Cu half-cells in different carbon-based electrolytes. (b) Coulombic efficiency of Li-Cu half-cells in different ether-based electrolytes. (c) Different morphologies of Li deposited on Cu foil under different electrolyte conditions [45]. Copyright 2015, Springer Nature. (d) SEM morphology and optical images (inset) of Li plating on Cu collector in 1:2 LiFSI-TEP electrolyte(left); Nail penetration test for 18650 cells were carried out with different electrolytes(right): A blank cell before the nail test(top), 1:2 LiFSI-TEP + FEC-LiBOB electrolyte (middle), 1.0 M LiPF<sub>6</sub>/EC:DEC:EMC=1:1:1 electrolyte (bottom) [82]. Copyright 2018, Springer Nature.

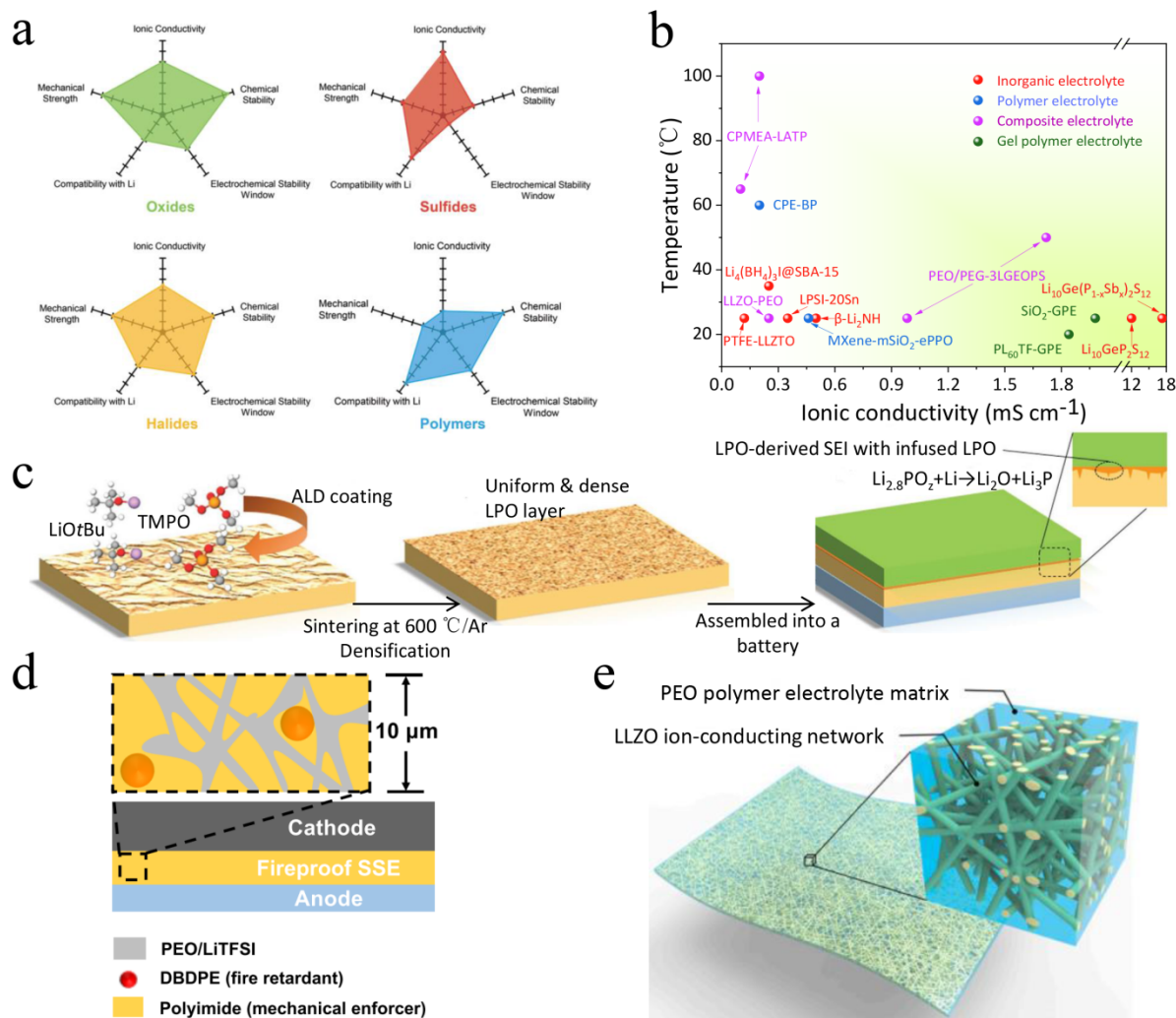


**Fig. 7.** (a) Radar charts of various solid electrolyte properties [6]. Copyright 2020, Royal Society of Chemistry. (b) Ionic conductivity of different solid electrolytes. (c) Schematic diagram of interface design for LLZTO with dense SEI membrane [46]. (d) Structure of PI/DBDPE/PEO/LiTFSI polymer solid electrolyte [108]. Copyright 2020, American Chemical Society. (e) Schematic diagram of LLZO/PEO composite solid electrolyte structure [100]. Copyright 2016, PNAS.

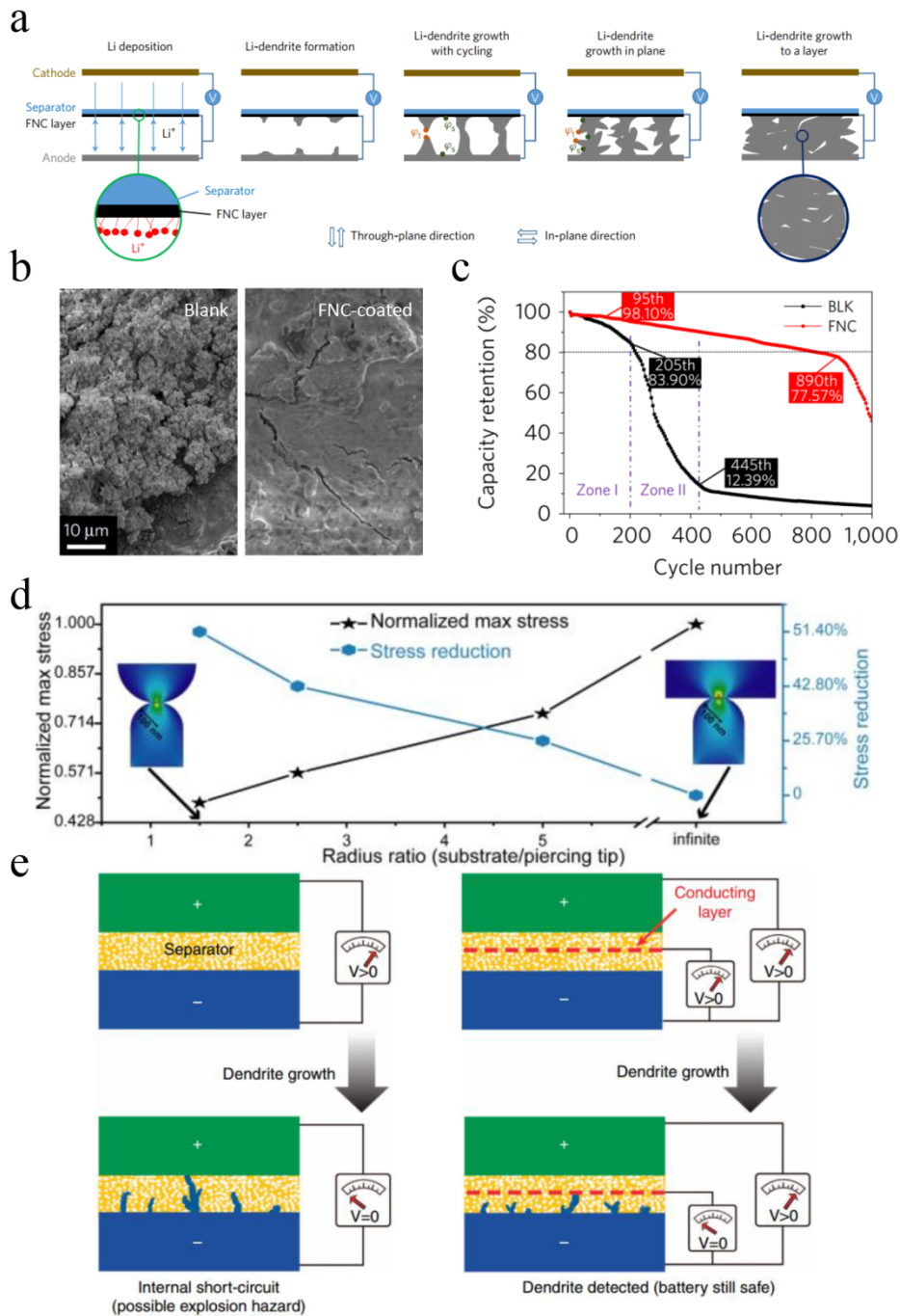


**Fig. 8.** (a) Li dendrites growth with FNC coated separator. (b) SEM images of the Li metal anode facing the blank separator and the FNC coated separator after the first charge at 1C (c) Capacity retention of Li/LiFePO<sub>4</sub> cells using the FNC coated separator [39]. Copyright 2017, Springer Nature. (d) Diagram of the relationship between surface radius ratios and stress when penetrated by a tip [125]. Copyright 2020, Wiley. (e) Schematic diagram of modified separator for monitoring dendrites growth [122]. Copyright 2014, Springer Nature.

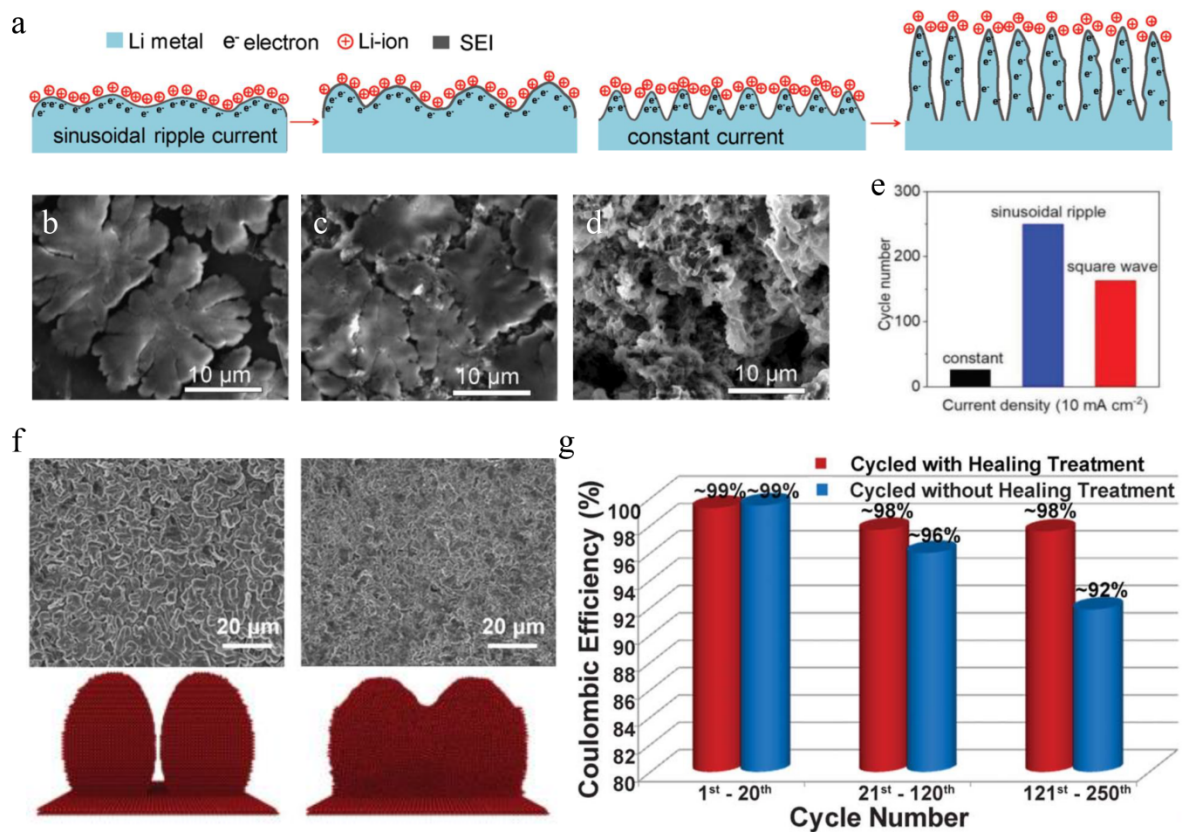


**Fig. 9.** (a) Different growth models of Li dendrites under sinusoidal ripple current and constant current. (b-d) Surface morphologies of Li after 10 cycles of different charging strategies at  $10 \text{ mA cm}^{-2}$  (b: sinusoidal ripple current; c: square wave current; d: constant current). (e) Number of cycles of the battery under different charging strategies [38]. Copyright 2019, Wiley. (f) Li surface morphology before and after self-healing and simulation screenshot of self-healing. (g) Comparison of Coulombic efficiency with and without healing treatment in Li-S full battery [132]. Copyright 2018, National Academy of Sciences.

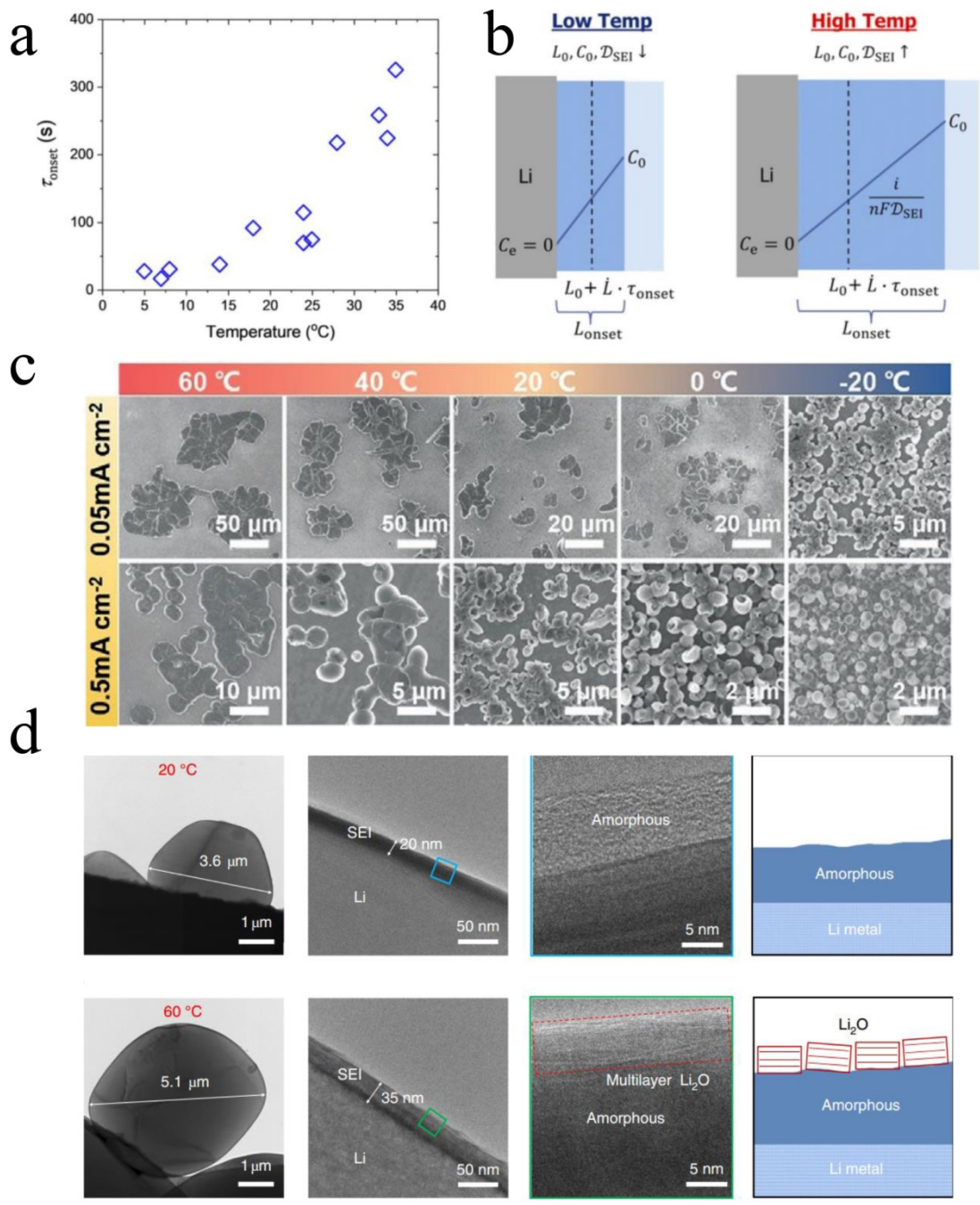


**Fig. 10.** (a) Relationship between dendrites onset time and Li plating temperature (b) Schematic of the effect of different temperatures on the thickness of SEI on the surface of Li [134]. Copyright 2019, Wiley. (c) SEM images of Li nuclei layers at varied current densities and temperature conditions. [136]. Reproduced from ref.149. Copyright 2019, Wiley. (d) Cryo-electron microscopy to observe the structure of SEI film at varied temperature [137]. Copyright 2019, Springer Nature.

**Table1.** Recent progress of LMBs modified with different materials.

Materials	Current density (mA cm <sup>-2</sup> )	Capacity (mAh cm <sup>-2</sup> )	Cycle time (h)	Electrolytes	Remarks	References
Carbon paper/Sn/SnO <sub>2</sub>	1	1	800	1 M LiTFSI in 1:1 DOL/DME +1 wt. % LiNO <sub>3</sub>	Composite anode	47
Lamellar structured Ti <sub>3</sub> C <sub>2</sub> MXene	1	1	400	1 M LiPF <sub>6</sub> in 1:1 EC/DMC	Composite anode	48
Layered Li-rGO composite film	1	1	880	1 M LiTFSI in 1:1 DOL/DME +1 wt. % LiNO <sub>3</sub>	Composite anode	49
3D Cu mesh	0.5	1	1200	1 M LiTFSI in 1:1 DOL/DME+1 wt. % LiNO <sub>3</sub>	3D Current collector	50
Vertically oriented Li-Cu-Li arrays	1	5	800	1 M LiPF <sub>6</sub> in 1:1 EC/EMC/DEC + 1 wt. % VC	3D Current collector	51
Li-In alloy	2	1	>1000	1 M LiTFSI in 1:1 DOL/DME	Alloy anode	23
Mg Doped Li-LiB Alloy	0.5	0.5	500	1 M LiPF <sub>6</sub> in 1:1:1 EC/DMC/EMC+VC	Alloy anode	52
3D PMF/Li Composite Anode	2	1	350	1 M LiTFSI in 1:1 DOL/DME +2 wt. % LiNO <sub>3</sub>	Li surface protection	36
Parallely Aligned MXene Layers-Li	1	35	400	1 M LiPF <sub>6</sub> in 1:1:1 EC /EMC/DMC	Li surface protection	53
Li <sub>2</sub> S/Li <sub>2</sub> Se protection layer	1.5	3	900	1 M LiTFSI in 1:1 DOL/DME+1 wt. % LiNO <sub>3</sub>	Li surface protection	54
Li <sub>2</sub> S protection layer	5	2	750	1 M LiTFSI in 1:1 DOL/DME	Li surface protection	27
Trifluoroethanol-modified eggshell	10	5	700	1 M LiTFSI in 1:1 DOL/DME+1 wt. % LiNO <sub>3</sub>	Modified current collector	55

## References

- [1] J.W. Choi, D. Aurbach, Promise and reality of post-lithium-ion batteries with high energy densities, *Nat. Rev. Mater.* 1 (2016) 16013, <https://doi.org/10.1038/natrevmats.2016.13>.
- [2] C. Liu, F. Li, L.P. Ma, H.M. Cheng, Advanced materials for energy storage, *Adv. Mater.* 22 (2010) E28-E62, <https://doi.org/10.1002/adma.200903328>.
- [3] B. Dunn, H. Kamath, J.M. Tarascon, Electrical energy storage for the grid: a battery of choices, *Science* 334 (2011) 928-935, <https://doi.org/10.1126/science.1212741>.
- [4] E.C. Evarts, Lithium batteries to the limits of lithium, *Nature* 526 (2015) S93-S95, <https://doi.org/10.1038/526S93a>.
- [5] M. Armand, J.M. Tarascon, Building better batteries, *Nature* 451 (2008) 652-657, <https://doi.org/10.1038/451652a>.
- [6] X. Zhang, Y.A. Yang, Z. Zhou, Towards practical lithium-metal anodes, *Chem. Soc. Rev.* 49 (2020) 3040-3071, <https://doi.org/10.1039/c9cs00838a>.
- [7] B. Liu, J.G. Zhang, G.Z. Shen, Pursuing two-dimensional nanomaterials for flexible lithium-ion batteries, *Nano Today* 11 (2016) 82-97, <https://doi.org/10.1016/j.nantod.2016.02.003>.
- [8] F.X. Wu, J. Maier, Y. Yu, Guidelines and trends for next-generation rechargeable lithium and lithium-ion batteries, *Chem. Soc. Rev.* 49 (2020) 1569-1614, <https://doi.org/10.1039/c7cs00863e>.
- [9] W. Xu, J.L. Wang, F. Ding, X.L. Chen, E. Nasybutin, Y.H. Zhang, J.G. Zhang, Lithium metal anodes for rechargeable batteries, *Energy Environ. Sci.* 7 (2014) 513-537, <https://doi.org/10.1039/c3ee40795k>.
- [10] G. Jiang, K. Li, J. Mao, N. Jiang, J. Luo, G. Ding, Y. Li, F. Sun, B. Dai, Y. Li, Sandwich-like prussian blue/graphene oxide composite films as ion-sieves for fast and uniform Li ionic flux in highly stable Li metal batteries, *Chem. Eng. J.* 385 (2020) 123398,

<https://doi.org/10.1016/j.cej.2019.123398>.

[11] Y.J. Oh, J.H. Kim, J.Y. Lee, S.-K. Park, Y.C. Kang, Design of house centipede-like MoC–Mo<sub>2</sub>C nanorods grafted with N-doped carbon nanotubes as bifunctional catalysts for high-performance Li–O<sub>2</sub> batteries, *Chem. Eng. J.* 384 (2020) 123344, <https://doi.org/10.1016/j.cej.2019.123344>.

[12] A. Manthiram, Y.Z. Fu, S.H. Chung, C.X. Zu, Y.S. Su, Rechargeable lithium-sulfur batteries, *Chem. Rev.* 114 (2014) 11751-11787, <https://doi.org/10.1021/cr500062v>.

[13] F. Hao, A. Verma, P.P. Mukherjee, Mechanistic insight into dendrite-SEI interactions for lithium metal electrodes, *J. Mater. Chem. A* 6 (2018) 19664-19671, <https://doi.org/10.1039/c8ta07997h>.

[14] D.C. Lin, Y.Y. Liu, Y. Cui, Reviving the lithium metal anode for high-energy batteries, *Nat. Nanotechnol.* 12 (2017) 194-206, <https://doi.org/10.1038/nnano.2017.16>.

[15] Z.A. Ghazi, Z.H. Sun, C.G. Sun, F.L. Qi, B.G. An, F. Li, H.M. Cheng, Key aspects of lithium metal anodes for lithium metal batteries, *Small* 15 (2019) 1900687, <https://doi.org/10.1002/sml.201900687>.

[16] J.M. Tarascon, M. Armand, Issues and challenges facing rechargeable lithium batteries, *Nature* 414 (2001) 359-367, <https://doi.org/10.1038/35104644>.

[17] X.Z. Guan, A.X. Wang, S. Liu, G.J. Li, F. Liang, Y.W. Yang, X.J. Liu, J.Y. Luo, Controlling nucleation in lithium metal anodes, *Small* 14 (2018) 1801423, <https://doi.org/10.1002/sml.201801423>.

[18] Y.Z. Li, Y.B. Li, Y.M. Sun, B. Butz, K. Yan, A.L. Koh, J. Zhao, A. Pei, Y. Cui, Revealing nanoscale passivation and corrosion mechanisms of reactive battery materials in gas environments, *Nano Lett.* 17 (2017) 5171-5178, <https://doi.org/10.1021/acs.nanolett.7b02630>.

[19] C. Zheng, Y. Ruan, J. Su, Z. Song, T. Xiu, J. Jin, M.E. Badding, Z. Wen, Grain boundary

modification in garnet electrolyte to suppress lithium dendrite growth, *Chem. Eng. J.* 411 (2021) 128508, <https://doi.org/10.1016/j.cej.2021.128508>.

[20] Z. Xie, Z. Wua, X. An, X. Yue, A. Yoshida, X. Du, X. Hao, A. Abudula, G. Guan, 2-Fluoropyridine: a novel electrolyte additive for lithium metal batteries with high areal capacity as well as high cycling stability, *Chem. Eng. J.* 393 (2020) 124789, <https://doi.org/10.1016/j.cej.2020.124789>.

[21] X.B. Cheng, R. Zhang, C.Z. Zhao, Q. Zhang, Toward safe lithium metal anode in rechargeable batteries: a review, *Chem. Rev.* 117 (2017) 10403-10473, <https://doi.org/10.1021/acs.chemrev.7b00115>.

[22] S.H. Choi, S.J. Lee, D.J. Yoo, J.H. Park, J.H. Park, Y.N. Ko, J. Park, Y.E. Sung, S.Y. Chung, H. Kim, J.W. Choi, Marginal magnesium doping for high-performance lithium metal batteries, *Adv. Energy Mater.* 9 (2019) 1902278, <https://doi.org/10.1002/aenm.201902278>.

[23] X. Liang, Q. Pang, I.R. Kochetkov, M.S. Sempere, H. Huang, X.Q. Sun, L.F. Nazar, A facile surface chemistry route to a stabilized lithium metal anode, *Nat. Energy* 2 (2017) 17119, <https://doi.org/10.1038/nenergy.2017.119>.

[24] S. Liu, L. Deng, W. Guo, C. Zhang, X. Liu, J. Luo, Bulk nanostructured materials design for fracture resistant lithium metal anodes, *Adv. Mater.* 31 (2019) 1807585, <https://doi.org/10.1002/adma.201807585>.

[25] H. Ye, Z.J. Zheng, H.R. Yao, S.C. Liu, T.T. Zuo, X.W. Wu, Y.X. Yin, N.W. Li, J.J. Gu, F.F. Cao, Y.G. Guo, Guiding uniform Li plating/stripping through lithium-aluminum alloying medium for long-life Li metal batteries, *Angew. Chem. Int. Ed.* 58 (2019) 1094-1099, <https://doi.org/10.1002/anie.201811955>.

[26] S.F. Liu, X. Ji, J. Yue, S. Hou, P.F. Wang, C.Y. Cui, J. Chen, B.W. Shao, J.R. Li, F.D. Han, J.P. Tu, C.S. Wang, High interfacial-energy interphase promoting safe lithium metal batteries, *J. Am. Chem. Soc.* 142 (2020) 2438-2447, <https://doi.org/10.1021/jacs.9b11750>.

- [27] H. Chen, A. Pei, D.C. Lin, J. Xie, A.K. Yang, J.W. Xu, K.X. Lin, J.Y. Wang, H.S. Wang, F.F. Shi, D. Boyle, Y. Cui, Uniform high ionic conducting lithium sulfide protection layer for stable lithium metal anode, *Adv. Energy Mater.* 9 (2019) 1900858, <https://doi.org/10.1002/aenm.201900858>.
- [28] S. Sun, S. Myung, G. Kim, D. Lee, H. Son, M. Jang, E. Park, B. Son, Y.-G. Jung, U. Paik, T. Song, Facile ex situ formation of a LiF–polymer composite layer as an artificial SEI layer on Li metal by simple roll-press processing for carbonate electrolyte-based Li metal batteries, *J. Mater. Chem. A* 8 (2020) 17229–17237, <https://doi.org/10.1039/D0TA05372D>.
- [29] Y. Yang, J. Xiong, S. Lai, R. Zhou, M. Zhao, H. Geng, Y. Zhang, Y. Fang, C. Li, J. Zhao, Vinyl ethylene carbonate as an effective SEI-forming additive in carbonate-based electrolyte for lithium-metal anodes, *ACS Appl. Mater. Interfaces* 11 (2019) 6118–6125, <https://doi.org/10.1021/acsami.8b20706>.
- [30] L. Wang, R. Xie, B. Chen, X. Yu, J. Ma, C. Li, Z. Hu, X. Sun, C. Xu, S. Dong, T.-S. Chan, J. Luo, G. Cui, L. Chen, In-situ visualization of the space-charge-layer effect on interfacial lithium-ion transport in all-solid-state batteries, *Nat. Commun.* 11 (2020) 5889, <https://doi.org/10.1038/s41467-020-19726-5>.
- [31] A.M. Hafez, J. Sheng, D. Cao, Y. Chen, H. Zhu, Flexible lithium metal anode featuring ultrahigh current density stability with uniform deposition and dissolution, *ES Energy Environ.* 5 (2019) 85–93, <https://doi.org/10.30919/esee8c311>.
- [32] X. Chen, X.-R. Chen, T.-Z. Hou, B.-Q. Li, X.-B. Cheng, R. Zhang, Q. Zhang, Lithiophilicity chemistry of heteroatom-doped carbon to guide uniform lithium nucleation in lithium metal anodes, *Sci. Adv.* 5 (2019) eaau7728, <https://doi.org/10.1126/sciadv.aau7728>.
- [33] X. Wang, W. Zeng, L. Hong, W. Xu, H. Yang, F. Wang, H. Duan, M. Tang, H. Jiang, Stress-driven lithium dendrite growth mechanism and dendrite mitigation by electroplating on soft substrates, *Nat. Energy* 3 (2018) 227–235, <https://doi.org/10.1038/s41560-018-0104-5>.

- [34] A. Wang, S. Tang, D. Kong, S. Liu, K. Chiou, L. Zhi, J. Huang, Y.-Y. Xia, J. Luo, Bending-tolerant anodes for lithium-metal batteries, *Adv. Mater.* 30 (2018) 1703891, <https://doi.org/10.1002/adma.201703891>.
- [35] J. Pu, J.C. Li, K. Zhang, T. Zhang, C.W. Li, H.X. Ma, J. Zhu, P.V. Braun, J. Lu, H.G. Zhang, Conductivity and lithiophilicity gradients guide lithium deposition to mitigate short circuits, *Nat. Commun.* 10 (2019) 1896, <https://doi.org/10.1038/s41467-019-09932-1>.
- [36] L. Fan, H.L. Zhuang, W.D. Zhang, Y. Fu, Z.H. Liao, Y.Y. Lu, Stable lithium electrodeposition at ultra-high current densities enabled by 3D PMF/Li composite anode, *Adv. Energy Mater.* 8 (2018) 1703360, <https://doi.org/10.1002/aenm.201703360>.
- [37] Q. Li, S. Tan, L.L. Li, Y.Y. Lu, Y. He, Understanding the molecular mechanism of pulse current charging for stable lithium metal batteries., *Sci. Adv.* 3 (2017) e1701246, <https://doi.org/10.1126/sciadv.1701246>.
- [38] Z.L. Zhang, Z.L. Wang, X.M. Lu, Suppressing lithium dendrite growth via sinusoidal ripple current produced by triboelectric nanogenerators, *Adv. Energy Mater.* 9 (2019) 1900487, <https://doi.org/10.1002/aenm.201900487>.
- [39] Y.D. Liu, Q. Liu, L. Xin, Y.Z. Liu, F. Yang, E.A. Stach, J. Xie, Making Li metal electrodes rechargeable by controlling the dendrite growth direction, *Nat. Energy* 2 (2017) 17083, <https://doi.org/10.1038/nenergy.2017.83>.
- [40] E. Peled, The electrochemical behavior of alkali and alkaline earth metals in nonaqueous battery systems-the solid electrolyte interphase model, *J. Electrochem. Soc.* 126 (1979) 2047-2051, <https://doi.org/10.1149/1.2128859>.
- [41] S.Z. Xiong, K. Xie, Y. Diao, X.B. Hong, Properties of surface film on lithium anode with LiNO<sub>3</sub> as lithium salt in electrolyte solution for lithium-sulfur batteries, *Electrochim. Acta* 83 (2012) 78-86, <https://doi.org/10.1016/j.electacta.2012.07.118>.
- [42] X.B. Cheng, R. Zhang, C.Z. Zhao, F. Wei, J.G. Zhang, Q. Zhang, A review of solid

electrolyte interphases on lithium metal anode, *Adv. Sci.* 3 (2016) 1500213, <https://doi.org/10.1002/advs.201500213>.

[43] Z. Peng, X. Cao, P.Y. Gao, H.P. Jia, X.D. Ren, S. Roy, Z.D. Li, Y. Zhu, W.P. Xie, D.Y. Liu, Q.Y. Li, D.Y. Wang, W. Xu, J.G. Zhang, High power lithium metal batteries enabled by high concentration acetonitrile based electrolytes with vinylene carbonate additive, *Adv. Funct. Mater.* 30 (2020) 2001285, <https://doi.org/10.1002/adfm.202001285>.

[44] R. Pathak, K. Chen, A. Gurung, K.M. Reza, B. Bahrami, J. Pokharel, A. Baniya, W. He, F. Wu, Y. Zhou, K. Xu, Q.Q. Qiao, Fluorinated hybrid solid-electrolyte-interphase for dendrite-free lithium deposition, *Nat. Commun.* 11 (2020) 93, <https://doi.org/10.1038/s41467-019-13774-2>.

[45] J.F. Qian, W.A. Henderson, W. Xu, P. Bhattacharya, M. Engelhard, O. Borodin, J.G. Zhang, High rate and stable cycling of lithium metal anode, *Nat. Commun.* 6 (2015) 6362, <https://doi.org/10.1038/ncomms7362>.

[46] T. Deng, X. Ji, Y. Zhao, L.S. Cao, S. Li, S. Hwang, C. Luo, P.F. Wang, H.P. Jia, X.L. Fan, X.C. Lu, D. Su, X.L. Sun, C.S. Wang, J.G. Zhang, Tuning the anode-electrolyte interface chemistry for garnet-based solid-state Li metal batteries, *Adv. Mater.* 32 (2020) 2000030, <https://doi.org/10.1002/adma.202000030>.

[47] L. Tan, S. Feng, X. Li, Z. Wang, W. Peng, T. Liu, G. Yan, L. Li, F. Wu, J. Wang, Oxygen-induced lithiophilicity of tin-based framework toward highly stable lithium metal anode, *Chem. Eng. J.* 394 (2020) 124848, <https://doi.org/10.1016/j.cej.2020.124848>.

[48] B. Li, D. Zhang, Y. Liu, Y.X. Yu, S.M. Li, S.B. Yang, Flexible  $Ti_3C_2$  MXene-lithium film with lamellar structure for ultrastable metallic lithium anodes, *Nano Energy* 39 (2017) 654-661, <https://doi.org/10.1016/j.nanoen.2017.07.023>.

[49] D.C. Lin, Y.Y. Liu, Z. Liang, H.W. Lee, J. Sun, H.T. Wang, K. Yan, J. Xie, Y. Cui, Layered reduced graphene oxide with nanoscale interlayer gaps as a stable host for lithium

- metal anodes, *Nat. Nanotechnol.* 11 (2016) 626-632, <https://doi.org/10.1038/nnano.2016.32>.
- [50] Q. Li, S.P. Zhu, Y.Y. Lu, 3D porous Cu current collector/Li-metal composite anode for stable lithium-metal batteries, *Adv. Funct. Mater.* 27 (2017) 1606422, <https://doi.org/10.1002/adfm.201606422>.
- [51] Z.J. Cao, B. Li, S.B. Yang, Dendrite-free lithium anodes with ultra-deep stripping and plating properties based on vertically oriented lithium-copper-lithium arrays, *Adv. Mater.* 31 (2019) 1901310, <https://doi.org/10.1002/adma.201901310>.
- [52] C. Wu, H.F. Huang, W.Y. Lu, Z.X. Wei, X.Y. Ni, F. Sun, P. Qing, Z.J. Liu, J.M. Ma, W.F. Wei, L.B. Chen, C.L. Yan, L.Q. Mai, Mg doped Li-LiB alloy with in situ formed lithiophilic LiB skeleton for lithium metal batteries, *Adv. Sci.* 7 (2020) 1902643, <https://doi.org/10.1002/advs.201902643>.
- [53] D. Zhang, S. Wang, B. Li, Y.J. Gong, S.B. Yang, Horizontal growth of lithium on parallelly aligned MXene layers towards dendrite-free metallic lithium anodes, *Adv. Mater.* 31 (2019) 1901820, <https://doi.org/10.1002/adma.201901820>.
- [54] F.F. Liu, L.F. Wang, Z.W. Zhang, P.C. Shi, Y.Z. Feng, Y. Yao, S.F. Ye, H.Y. Wang, X.J. Wu, Y. Yu, A mixed lithium-ion conductive  $\text{Li}_2\text{S}/\text{Li}_2\text{Se}$  protection layer for stable lithium metal anode, *Adv. Funct. Mater.* 30 (2020) 2001607, <https://doi.org/10.1002/adfm.202001607>.
- [55] Z.J. Ju, J.W. Nai, Y. Wang, T.F. Liu, J.H. Zheng, H.D. Yuan, O.W. Sheng, C.B. Jin, W.K. Zhang, Z. Jin, H. Tian, Y.J. Liu, X.Y. Tao, Biomacromolecules enabled dendrite-free lithium metal battery and its origin revealed by cryo-electron microscopy, *Nat. Commun.* 11 (2020) 488, <https://doi.org/10.1038/s41467-020-14358-1>.
- [56] H.M. Zhang, X.B. Liao, Y.P. Guan, Y. Xiang, M. Li, W.F. Zhang, X.Y. Zhu, H. Ming, L. Lu, J.Y. Qiu, Y.Q. Huang, G.P. Cao, Y.S. Yang, L.Q. Mai, Y. Zhao, H. Zhang, Lithiophilic-lithiophobic gradient interfacial layer for a highly stable lithium metal anode,

Nat. Commun. 9 (2018) 3729, <https://doi.org/10.1038/s41467-018-06126-z>.

[57] C.J. Niu, H.L. Pan, W. Xu, J. Xiao, J.G. Zhang, L.L. Luo, C.M. Wang, D.H. Mei, J.S. Meng, X.P. Wang, Z. Liu, L.Q. Mai, J. Liu, Self-smoothing anode for achieving high-energy lithium metal batteries under realistic conditions, Nat. Nanotechnol. 14 (2019) 594-601, <https://doi.org/10.1038/s41565-019-0427-9>.

[58] C. Zhang, S. Liu, G. Li, C. Zhang, X. Liu, J. Luo, Incorporating ionic paths into 3D conducting scaffolds for high volumetric and areal capacity, high rate lithium-metal anodes, Adv. Mater. 30 (2018) 1801328, <https://doi.org/10.1002/adma.201801328>.

[59] L.L. Kong, L. Wang, Z.C. Ni, S. Liu, G.R. Li, X.P. Gao, Lithium-magnesium alloy as a stable anode for lithium-sulfur battery, Adv. Funct. Mater. 29 (2019) 1808756, <https://doi.org/10.1002/adfm.201808756>.

[60] M.T. Wan, S.J. Kang, L. Wang, H.W. Lee, G.W. Zheng, Y. Cui, Y.M. Sun, Mechanical rolling formation of interpenetrated lithium metal/lithium tin alloy foil for ultrahigh-rate battery anode, Nat. Commun. 11 (2020) 829, <https://doi.org/10.1038/s41467-020-14550-3>.

[61] J.L. Ma, F.L. Meng, Y. Yu, D.P. Liu, J.M. Yan, Y. Zhang, X.B. Zhang, Q. Jiang, Prevention of dendrite growth and volume expansion to give high-performance aprotic bimetallic Li-Na alloy-O<sub>2</sub> batteries, Nat. Chem. 11 (2019) 64-70, <https://doi.org/10.1038/s41557-018-0166-9>.

[62] C.H. Chang, S.H. Chung, A. Manthiram, Dendrite-free lithium anode via a homogenous Li-ion distribution enabled by a kimwipe paper, Adv. Sustain. Syst. 1 (2017) 1600034, <https://doi.org/10.1002/adsu.201600034>.

[63] G.X. Li, Z. Liu, Q.Q. Huang, Y. Gao, M. Regula, D.W. Wang, L.Q. Chen, D.H. Wang, Stable metal battery anodes enabled by polyethylenimine sponge hosts by way of electrokinetic effects, Nat. Energy 3 (2018) 1076-1083, <https://doi.org/10.1038/s41560-018-0276-z>.

- [64] N.W. Li, Y. Shi, Y.X. Yin, X.X. Zeng, J.Y. Li, C.J. Li, L.J. Wan, R. Wen, Y.G. Guo, A flexible solid electrolyte interphase layer for long-life lithium metal anodes, *Angew. Chem. Int. Ed.* 57 (2018) 1505-1509, <https://doi.org/10.1002/anie.201710806>.
- [65] H.Y. Zhou, S.C. Yu, H.D. Liu, P. Liu, Protective coatings for lithium metal anodes: recent progress and future perspectives, *J. Power Sources* 450 (2020) 227632, <https://doi.org/10.1016/j.jpowsour.2019.227632>.
- [66] J.I. Lee, G. Song, S. Cho, D.Y. Han, S. Park, Lithium metal interface modification for high - energy batteries: approaches and characterization, *Batteries Supercaps* 3 (2020) 828-859, <https://doi.org/10.1002/batt.202000016>.
- [67] H. Duan, W.P. Chen, M. Fan, W.P. Wang, L. Yu, S.J. Tan, X. Chen, Q. Zhang, S. Xin, L.J. Wan, Y.G. Guo, Building an air stable and lithium deposition regulable garnet interface from moderate-temperature conversion chemistry, *Angew. Chem. Int. Ed.* 59 (2020) 12069-12075, <https://doi.org/10.1002/anie.202003177>.
- [68] H.D. Yuan, J.W. Nai, H. Tian, Z.J. Ju, W.K. Zhang, Y.J. Liu, X.Y. Tao, X.W. Lou, An ultrastable lithium metal anode enabled by designed metal fluoride spansules, *Sci. Adv.* 6 (2020) eaaz3112, <https://doi.org/10.1126/sciadv.aaz3112>.
- [69] Y.Z. Li, Y.B. Li, A.L. Pei, K. Yan, Y.M. Sun, C.L. Wu, L.M. Joubert, R. Chin, A.L. Koh, Y. Yu, J. Perrino, B. Butz, S. Chu, Y. Cui, Atomic structure of sensitive battery materials and interfaces revealed by cryo-electron microscopy, *Science* 358 (2017) 506-510, <https://doi.org/10.1126/science.aam6014>.
- [70] J.B. Goodenough, Y. Kim, Challenges for rechargeable Li batteries, *Chem. Mater.* 22 (2010) 587-603, <https://doi.org/10.1021/cm901452z>.
- [71] Y. Jie, X. Ren, R. Cao, W. Cai, S. Jiao, Advanced liquid electrolytes for rechargeable Li metal batteries, *Adv. Funct. Mater.* 30 (2020) 1910777, <https://doi.org/10.1002/adfm.201910777>.

- [72] S.H. Jiao, X.D. Ren, R.G. Cao, M.H. Engelhard, Y.Z. Liu, D.H. Hu, D.H. Mei, J.M. Zheng, W.G. Zhao, Q.Y. Li, N. Liu, B.D. Adams, C. Ma, J. Liu, J.G. Zhang, W. Xu, Stable cycling of high-voltage lithium metal batteries in ether electrolytes, *Nat. Energy* 3 (2018) 739-746, <https://doi.org/10.1038/s41560-018-0199-8>.
- [73] F. Ding, W. Xu, X.L. Chen, J. Zhang, M.H. Engelhard, Y.H. Zhang, B.R. Johnson, J.V. Crum, T.A. Blake, X.J. Liu, J.G. Zhang, Effects of carbonate solvents and lithium salts on morphology and coulombic efficiency of lithium electrode, *J. Electrochem. Soc.* 160 (2013) A1894-A1901, <https://doi.org/10.1149/2.100310jes>.
- [74] W.D. Zhang, Q. Wu, J.X. Huang, L. Fan, Z.Y. Shen, Y. He, Q. Feng, G.N. Zhu, Y.Y. Lu, Colossal granular lithium deposits enabled by the grain-coarsening effect for high-efficiency lithium metal full batteries, *Adv. Mater.* 32 (2020) 2001740, <https://doi.org/10.1002/adma.202001740>.
- [75] W. Li, H. Yao, K. Yan, G. Zheng, Z. Liang, Y.M. Chiang, Y. Cui, The synergetic effect of lithium polysulfide and lithium nitrate to prevent lithium dendrite growth, *Nat. Commun.* 6 (2015) 7436, <https://doi.org/10.1038/ncomms8436>.
- [76] H.P. Wu, Y. Cao, L.X. Geng, C. Wang, In situ formation of stable interfacial coating for high performance lithium metal anodes, *Chem. Mater.* 29 (2017) 3572-3579, <https://doi.org/10.1021/acs.chemmater.6b05475>.
- [77] Q. Wang, C.K. Yang, J.J. Yang, K. Wu, C.J. Hu, J. Lu, W. Liu, X.M. Sun, J.Y. Qiu, H.H. Zhou, Dendrite-free lithium deposition via a superfilling mechanism for high-performance Li-metal batteries, *Adv. Mater.* 31 (2019) 1903248, <https://doi.org/10.1002/adma.201903248>.
- [78] E. Markevich, G. Salitra, F. Chesneau, M. Schmidt, D. Aurbach, Very stable lithium metal stripping-plating at a high rate and high areal capacity in fluoroethylene carbonate-based organic electrolyte solution, *ACS Energy Lett.* 2 (2017) 1321-1326, <https://doi.org/10.1021/acsenergylett.7b00300>.

- [79] C. Brissot, M. Rosso, J.N. Chazalviel, S. Lascaud, Dendritic growth mechanisms in lithium/polymer cells, *J. Power Sources* 81 (1999) 925-929, [https://doi.org/10.1016/s0378-7753\(98\)00242-0](https://doi.org/10.1016/s0378-7753(98)00242-0).
- [80] X.L. Fan, L. Chen, X. Ji, T. Deng, S. Hou, J. Chen, J. Zheng, F. Wang, J.J. Jiang, K. Xu, C.S. Wang, Highly fluorinated interphases enable high-voltage Li-metal batteries, *Chem* 4 (2018) 174-185, <https://doi.org/10.1016/j.chempr.2017.10.017>.
- [81] C. Yan, X.B. Cheng, Y.X. Yao, X. Shen, B.Q. Li, W.J. Li, R. Zhang, J.Q. Huang, H. Li, Q. Zhang, An armored mixed conductor interphase on a dendrite-free lithium-metal anode, *Adv. Mater.* 30 (2018) 1804461, <https://doi.org/10.1002/adma.201804461>.
- [82] Z.Q. Zeng, V. Murugesan, K.S. Han, X.Y. Jiang, Y.L. Cao, L.F. Xiao, X.P. Ai, H.X. Yang, J.G. Zhang, M.L. Sushko, J. Liu, Non-flammable electrolytes with high salt-to-solvent ratios for Li-ion and Li-metal batteries, *Nat. Energy* 3 (2018) 674-681, <https://doi.org/10.1038/s41560-018-0196-y>.
- [83] S.-J. Tan, J. Yue, X.-C. Hu, Z.-Z. Shen, W.-P. Wang, J.-Y. Li, T.-T. Zuo, H. Duan, Y. Xiao, Y.-X. Yin, R. Wen, Y.-G. Guo, Nitriding-interface-regulated lithium plating enables flame retardant electrolytes for high-voltage lithium metal batteries, *Angew. Chem. Int. Ed.* 58 (2019) 7802-7807, <https://doi.org/10.1002/anie.201903466>.
- [84] S. Lee, K. Park, B. Koo, C. Park, M. Jang, H. Lee, H. Lee, Safe, stable cycling of lithium metal batteries with low-viscosity, fire-retardant locally concentrated ionic liquid electrolytes, *Adv. Funct. Mater.* 30 (2020) 2003132, <https://doi.org/10.1002/adfm.202003132>.
- [85] X.D. Ren, S.R. Chen, H. Lee, D.H. Mei, M.H. Engelhard, S.D. Burton, W.G. Zhao, J.M. Zheng, Q.Y. Li, M.S. Ding, M. Schroeder, J. Alvarado, K. Xu, Y.S. Meng, J. Liu, J.G. Zhang, W. Xu, Localized high-concentration sulfone electrolytes for high-efficiency lithium-metal batteries, *Chem* 4 (2018) 1877-1892, <https://doi.org/10.1016/j.chempr.2018.05.002>.
- [86] A. Manthiram, X.W. Yu, S.F. Wang, Lithium battery chemistries enabled by solid-state

- electrolytes, *Nat. Rev. Mater.* 2 (2017) 16103, <https://doi.org/10.1038/natrevmats.2016.103>.
- [87] Y.S. Hu, Getting solid, *Nat. Energy* 1 (2016) 16042, <https://doi.org/10.1038/nenergy.2016.42>.
- [88] L. Fan, S.Y. Wei, S.Y. Li, Q. Li, Y.Y. Lu, Recent progress of the solid-state electrolytes for high-energy metal-based batteries, *Adv. Energy Mater.* 8 (2018) 1702657, <https://doi.org/10.1002/aenm.201702657>.
- [89] T.L. Jiang, P.G. He, G.X. Wang, Y. Shen, C.W. Nan, L.Z. Fan, Solvent-free synthesis of thin, flexible, nonflammable garnet-based composite solid electrolyte for all-solid-state lithium batteries, *Adv. Energy Mater.* 10 (2020) 1903376, <https://doi.org/10.1002/aenm.201903376>.
- [90] B. Paik, A. Wolczyk, Lithium imide ( $\text{Li}_2\text{NH}$ ) as a solid-state electrolyte for electrochemical energy storage applications, *J. Phys. Chem. C* 123 (2019) 1619-1625, <https://doi.org/10.1021/acs.jpcc.8b10528>.
- [91] F.P. Zhao, J.W. Liang, C. Yu, Q. Sun, X.N. Li, K. Adair, C.H. Wang, Y. Zhao, S.M. Zhang, W.H. Li, S.X. Deng, R.Y. Li, Y.N. Huang, H. Huang, L. Zhang, S.Q. Zhao, S.G. Lu, X.L. Sun, A versatile Sn-substituted argyrodite sulfide electrolyte for all-solid-state Li metal batteries, *Adv. Energy Mater.* 10 (2020) 1903422, <https://doi.org/10.1002/aenm.201903422>.
- [92] J.W. Liang, N. Chen, X.N. Li, X. Li, K.R. Adair, J. Li, C.H. Wang, C. Yu, M.N. Banis, L. Zhang, S.Q. Zhao, S.G. Lu, H. Huang, R.Y. Li, Y.N. Huang, X.L. Sun,  $\text{Li}_{10}\text{Ge}(\text{P}_{1-x}\text{Sb}_x)_2\text{S}_{12}$  lithium-ion conductors with enhanced atmospheric stability, *Chem. Mater.* 32 (2020) 2664-2672, <https://doi.org/10.1021/acs.chemmater.9b04764>.
- [93] N. Kamaya, K. Homma, Y. Yamakawa, M. Hirayama, R. Kanno, M. Yonemura, T. Kamiyama, Y. Kato, S. Hama, K. Kawamoto, A. Mitsui, A lithium superionic conductor, *Nat. Mater.* 10 (2011) 682-686, <https://doi.org/10.1038/nmat3066>.
- [94] F.Q. Lu, Y.P. Pang, M.F. Zhu, F.D. Han, J.H. Yang, F. Fang, D.L. Sun, S.Y. Zheng, C.S.

Wang, A High-performance Li-B-H electrolyte for all-solid-state Li batteries, *Adv. Funct. Mater.* 29 (2019) 1809219, <https://doi.org/10.1002/adfm.201809219>.

[95] N. Wu, Y.T. Li, A. Dolocan, W. Li, H.H. Xu, B. Xu, N.S. Grundish, Z.M. Cui, H.B. Jin, J.B. Goodenough, In situ formation of Li<sub>3</sub>P layer enables fast Li<sup>+</sup> conduction across Li/solid polymer electrolyte interface, *Adv. Funct. Mater.* 30 (2020) 2000831, <https://doi.org/10.1002/adfm.202000831>.

[96] Y.Z. Shi, B. Li, Q. Zhu, K. Shen, W.J. Tang, Q. Xiang, W.H. Chen, C.T. Liu, J.Y. Luo, S.B. Yang, MXene-based mesoporous nanosheets toward superior lithium ion conductors, *Adv. Energy Mater.* 10 (2020) 1903534, <https://doi.org/10.1002/aenm.201903534>.

[97] P. Yang, X.W. Gao, X.L. Tian, C.Y. Shu, Y.K. Yi, P. Liu, T. Wang, L. Qu, B.B. Tian, M.T. Li, W. Tang, B.L. Yang, J.B. Goodenough, Upgrading traditional organic electrolytes toward future lithium metal batteries: A hierarchical nano-SiO<sub>2</sub>-supported gel polymer electrolyte, *ACS Energy Lett.* 5 (2020) 1681-1688, <https://doi.org/10.1021/acsenergylett.0c00412>.

[98] W.D. Zhou, S.F. Wang, Y.T. Li, S. Xin, A. Manthiram, J.B. Goodenough, Plating a dendrite-free lithium anode with a polymer/ceramic/polymer sandwich electrolyte, *J. Am. Chem. Soc.* 138 (2016) 9385-9388, <https://doi.org/10.1021/jacs.6b05341>.

[99] K.C. Pan, L. Zhang, W.W. Qian, X.K. Wu, K. Dong, H.T. Zhang, S.J. Zhang, A Flexible Ceramic/Polymer Hybrid Solid Electrolyte for Solid-State Lithium Metal Batteries, *Adv. Mater.* 32 (2020) 2000399, <https://doi.org/10.1002/adma.202000399>.

[100] K. Fu, Y.H. Gong, J.Q. Dai, A. Gong, X.G. Han, Y.G. Yao, C.W. Wang, Y.B. Wang, Y.N. Chen, C.Y. Yan, Y.J. Li, E.D. Wachsman, L.B. Hu, Flexible, solid-state, ion-conducting membrane with 3D garnet nanofiber networks for lithium batteries, *Proc. Natl. Acad. Sci. U.S.A.* 113 (2016) 7094-7099, <https://doi.org/10.1073/pnas.1600422113>.

[101] D. Xu, J.M. Su, J. Jin, C. Sun, Y.D. Ruan, C.H. Chen, Z.Y. Wen, In situ generated

fireproof gel polymer electrolyte with  $\text{Li}_{6.4}\text{Ga}_{0.2}\text{La}_3\text{Zr}_2\text{O}_{12}$  As initiator and ion conductive filler, *Adv. Energy Mater.* 9 (2019) 1900611, <https://doi.org/10.1002/aenm.201900611>.

[102] Z.Y. Jiang, H.Q. Xie, S. Wang, X. Song, X. Yao, H.H. Wang, Perovskite membranes with vertically aligned microchannels for all-solid-state lithium batteries, *Adv. Energy Mater.* 8 (2018) 1801433, <https://doi.org/10.1002/aenm.201801433>.

[103] T. Yoshinari, R. Koerver, P. Hofmann, Y. Uchimoto, W.G. Zeier, J. Janek, Interfacial stability of phosphate-NASICON solid electrolytes in Ni-rich NCM cathode-based solid-state batteries, *ACS Appl. Mater. Interfaces* 11 (2019) 23244-23253, <https://doi.org/10.1021/acsami.9b05995>.

[104] H.Y. Huo, X.N. Li, Y.P. Sun, X.T. Lin, K. Doyle-Davis, J.W. Liang, X.J. Gao, R.Y. Li, H. Huang, X.X. Guo, X.L. Sun,  $\text{Li}_2\text{CO}_3$  effects: New insights into polymer/garnet electrolytes for dendrite-free solid lithium batteries, *Nano Energy* 73 (2020) 104836, <https://doi.org/10.1016/j.nanoen.2020.104836>.

[105] H.Y. Huo, J. Luo, V. Thangadurai, X.X. Guo, C.W. Nan, X.L. Sun,  $\text{Li}_2\text{CO}_3$ : A critical issue for developing solid garnet batteries, *ACS Energy Lett.* 5 (2020) 252-262, <https://doi.org/10.1021/acsenergylett.9b02401>.

[106] Y. Zhu, J.G. Connell, S. Tepavcevic, P. Zapol, R. Garcia-Mendez, N.J. Taylor, J. Sakamoto, B.J. Ingram, L.A. Curtiss, J.W. Freeland, D.D. Fong, N.M. Markovic, Dopant-dependent stability of garnet solid electrolyte interfaces with lithium metal, *Adv. Energy Mater.* 9 (2019) 1803440, <https://doi.org/10.1002/aenm.201803440>.

[107] E. Quartarone, P. Mustarelli, Electrolytes for solid-state lithium rechargeable batteries: recent advances and perspectives, *Chem. Soc. Rev.* 40 (2011) 2525-2540, <https://doi.org/10.1039/c0cs00081g>.

[108] Y. Cui, J.Y. Wan, Y.S. Ye, K. Liu, L.Y. Chou, A fireproof, lightweight, polymer-polymer solid-state electrolyte for safe lithium batteries, *Nano Lett.* 20 (2020)

1686-1692, <https://doi.org/10.1021/acs.nanolett.9b04815>.

[109] Z.L. Hu, G.J. Li, A.X. Wang, J.Y. Luo, X.J. Liu, Recent progress of electrolyte design for lithium metal batteries, *Batteries Supercaps* 3 (2020) 331-335, <https://doi.org/10.1002/batt.201900191>.

[110] Y. Gao, Z.F. Yan, J.L. Gray, X. He, D.W. Wang, T.H. Chen, Q.Q. Huang, Y.C. Li, H.Y. Wang, S.H. Kim, T.E. Mallouk, D.H. Wang, Polymer-inorganic solid-electrolyte interphase for stable lithium metal batteries under lean electrolyte conditions, *Nat. Mater.* 18 (2019) 384-389, <https://doi.org/10.1038/s41563-019-0305-8>.

[111] A.L. Ahmad, U.R. Farooqui, N.A. Hamid, Effect of graphene oxide (GO) on poly(vinylidene fluoridehexafluoropropylene) (PVDF- HFP) polymer electrolyte membrane, *Poly* 142 (2018) 330e336, <https://doi.org/10.1016/j.polymer.2018.03.052>.

[112] Y.D. Pan, S.L. Chou, H.K. Liu, S.X. Dou, Functional membrane separators for next-generation high-energy rechargeable batteries, *Natl. Sci. Rev.* 4 (2017) 917-933, <https://doi.org/10.1093/nsr/nwx037>.

[113] S.S. Zhang, A review on the separators of liquid electrolyte Li ion batteries, *J. Power Sources* 164 (2007) 351-364, <https://doi.org/10.1016/j.jpowsour.2006.10.065>.

[114] H. Lee, X.D. Ren, C.J. Niu, L. Yu, M.H. Engelhard, I. Cho, M.H. Ryou, H.S. Jin, H.T. Kim, J. Liu, W. Xu, J.G. Zhang, Suppressing lithium dendrite growth by metallic coating on a separator, *Adv. Funct. Mater.* 27 (2017) 1704391, <https://doi.org/10.1002/adfm.201770266>.

[115] T. Zhang, J. Yang, Z.X. Xu, H.P. Li, Y.S. Guo, C.D. Liang, J.L. Wang, Suppressing dendrite growth of a lithium metal anode by modifying conventional polypropylene separators with a composite layer, *ACS Appl. Energy Mater.* 3 (2020) 506-513, <https://doi.org/10.1021/acsaem.9b01763>.

[116] X.F. Mao, L. Shi, H.J. Zhang, Z.Y. Wang, J.F. Zhu, Z.F. Qiu, Y. Zhao, M.H. Zhang, S. Yuan, Polyethylene separator activated by hybrid coating improving Li<sup>+</sup> ion transference

number and ionic conductivity for Li metal battery, *J. Power Sources* 342 (2017) 816-824, <https://doi.org/10.1016/j.jpowsour.2017.01.006>.

[117] Y.N. Wang, L.Y. Shi, H.L. Zhou, Z.Y. Wang, R. Li, J.F. Zhu, Z.F. Qiu, Y. Zhao, M.H. Zhang, S. Yuan, Polyethylene separators modified by ultrathin hybrid films enhancing lithium ion transport performance and Li metal anode stability, *Electrochim. Acta* 259 (2018) 386-394, <https://doi.org/10.1016/j.electacta.2017.10.120>.

[118] K. Liu, D. Zhuo, H.W. Lee, W. Liu, D.C. Lin, Y.Y. Lu, Y. Cui, Extending the life of lithium based rechargeable batteries by reaction of lithium dendrites with a novel silica nanoparticle sandwiched separator, *Adv. Mater.* 29 (2017) 1603987, <https://doi.org/10.1002/adma.201603987>.

[119] Y.R. Zhong, F. Lin, M.Y. Wang, Y.F. Zhang, Q. Ma, J. Lin, Z.X. Feng, H.L. Wang, Metal organic framework derivative improving lithium metal anode cycling, *Adv. Funct. Mater.* 30 (2020) 1907579, <https://doi.org/10.1002/adfm.201907579>.

[120] M.S. Gonzalez, Q.Z. Yan, J. Holoubek, Z.H. Wu, H.Y. Zhou, N. Patterson, V. Petrova, H.D. Liu, P. Liu, Draining over blocking: nano-composite janus separators for mitigating internal shorting of lithium batteries, *Adv. Mater.* 32 (2020) 1906836, <https://doi.org/10.1002/adma.201906836>.

[121] M.M. Chi, L. Shi, Z.Y. Wang, J.F. Zhu, X.F. Mao, Y. Zhao, M.H. Zhang, L.N. Sun, S. Yuan, Excellent rate capability and cycle life of Li metal batteries with ZrO<sub>2</sub>/POSS multilayer assembled PE separators, *Nano Energy* 28 (2016) 1-11, <https://doi.org/10.1016/j.nanoen.2016.07.037>.

[122] H. Wu, D. Zhuo, D.S. Kong, Y. Cui, Improving battery safety by early detection of internal shorting with a bifunctional separator, *Nat. Commun.* 5 (2014) 5193, <https://doi.org/10.1038/ncomms6193>.

[123] C. Monroe, J. Newman, The impact of elastic deformation on deposition kinetics at

lithium polymer interface, *J. Electrochem. Soc.* 152 (2005) A396-A404, <https://doi.org/10.1149/1.1850854>.

[124] X. Hao, J. Zhu, X. Jiang, H. Wu, J. Qiao, W. Sun, Z. Wang, K. Sun, Ultrastrong polyoxazole nanofiber membranes for dendrite-proof and heat-resistant battery separators, *Nano Lett.* 16 (2016) 2981-2987, <https://doi.org/10.1021/acs.nanolett.5b05133>.

[125] J. Liang, Q.Y. Chen, X.B. Liao, P.C. Yao, B. Zhu, G.X. Lv, X.Y. Wang, X. Chen, J. Zhu, A nano-shield design for separators to resist dendrite formation in lithium-metal batteries, *Angew. Chem. Int. Ed.* 59 (2020) 6561-6566, <https://doi.org/10.1002/anie.201915440>.

[126] T. Wang, R.V. Salvatierra, J.M. Tour, Detecting Li dendrites in a two electrode battery system, *Adv. Mater.* 31 (2019) 1807405, <https://doi.org/10.1002/adma.201807405>.

[127] A. Wang, Q. Deng, L. Deng, X. Guan, J. Luo, Eliminating tip dendrite growth by lorentz force for stable lithium metal anodes, *Adv. Funct. Mater.* 29 (2019) 1902630, <https://doi.org/10.1002/adfm.201902630>.

[128] M.A. Monem, K. Trad, N. Omar, O. Hegazy, B. Mantels, G. Mulder, P. Van den Bossche, J. Van Mierlo, Lithium-ion batteries: Evaluation study of different charging methodologies based on aging process, *Appl. Energy* 152 (2015) 143-155, <https://doi.org/10.1016/j.apenergy.2015.02.064>.

[129] S.Q. Zhu, C. Hu, Y. Xu, Y. Jin, J.L. Shui, Performance improvement of lithium ion battery by pulse current, *J. Energy Chem.* 46 (2020) 208-214, <https://doi.org/10.1016/j.jechem.2019.11.007>.

[130] A. Aryanfar, D. Brooks, B.V. Merinov, W.A. Goddard, III, A.J. Colussi, M.R. Hoffmann, Dynamics of lithium dendrite growth and inhibition: pulse charging experiments and monte carlo calculations, *J. Phys. Chem. Lett.* 5 (2014) 1721-1726, <https://doi.org/10.1021/jz500207a>.

- [131] I.W. Seong, C.H. Hong, B.K. Kim, W.Y. Yoon, The effects of current density and amount of discharge on dendrite formation in the lithium powder anode electrode, *J. Power Sources* 178 (2008) 769-773, <https://doi.org/10.1016/j.jpowsour.2007.12.062>.
- [132] L. Li, S. Basu, Y.P. Wang, Z.Z. Chen, P. Hundekar, B.W. Wang, J. Shi, Y.F. Shi, S. Narayanan, N. Koratkar, Self-heating-induced healing of lithium dendrites, *Science* 359 (2018) 1513-1516, <https://doi.org/10.1126/science.aap8787>.
- [133] Z.J. Hong, V. Viswanathan, Prospect of thermal shock induced healing of lithium dendrite, *ACS Energy Lett.* 4 (2019) 1012-1019, <https://doi.org/10.1021/acsenergylett.9b00433>.
- [134] A. Maraschky, R. Akolkar, Temperature dependence of dendritic lithium electrodeposition: a mechanistic study of the role of transport Li limitations within the SEI, *J. Electrochem. Soc.* 167 (2020) 062503, <https://doi.org/10.1149/1945-7111/ab7ce2>.
- [135] A.C. Thenuwara, P.P. Shetty, M.T. McDowell, Distinct nanoscale interphases and morphology of lithium metal electrodes operating at low temperatures, *Nano Lett.* 19 (2019) 8664-8672, <https://doi.org/10.1021/acs.nanolett.9b03330>.
- [136] K. Yan, J.Y. Wang, S.Q. Zhao, D. Zhou, B. Sun, Y. Cui, G.X. Wang, Temperature dependent nucleation and growth of dendrite free lithium metal anodes, *Angew. Chem. Int. Ed.* 58 (2019) 11364-11368, <https://doi.org/10.1002/anie.201905251>.
- [137] J.Y. Wang, W. Huang, A. Pei, Y.Z. Li, F.F. Shi, X.Y. Yu, Y. Cui, Improving cyclability of Li metal batteries at elevated temperatures and its origin revealed by cryo-electron microscopy, *Nat. Energy* 4 (2019) 664-670, <https://doi.org/10.1038/s41560-019-0413-3>.